



Investigating mechanical properties of
dissimilar welds of stainless steel 316L
and Inconel 625 for high temperature
corrosion applications

By

Daniel Shore

Supervised by

Reza Hashemi

Gunther Andersson

Completing the degree of

Bachelor of Science (chemical science) (honours), Masters of
Engineering (materials)
18 unit master's thesis

Flinders University
17/10/2022

Contents

List of Figures	2
List of Tables	5
List of Calculations	6
Abstract	7
DECLARATION	8
Acknowledgements	9
1. Introduction	10
1.1 Background	10
1.2 Definition of problem.....	11
1.2 Significance	12
1.3 Aims	12
2. Literature review.....	13
2.1 Individual points.....	13
2.2 Most relevant research	14
2.4 Gap in literature.....	16
3. Methodology	17
3.1 Sample preparation	17
3.1.1 welding process	17
3.1.2 Cutting processes	18
3.1.3 Polishing process.....	19
3.2 Testing details	19
3.2.1 Pristine	19
3.2.2 Argon heat treated.....	20
3.2.3 Air heat treated.....	20
3.2.4 Phase Changing Material heat treated (PCM)	21
3.3 Mechanical testing.....	21
3.3.1 Tensile stress testing	21
3.3.2 Vickers Hardness test	22
3.4 Characterisation.....	23
3.4.1 Optical microscopy.....	23
3.4.2 SEM and EDX analysis.....	24
4. Results.....	25
4.1 Tensile mechanical properties	25
4.2 Vickers hardness	29

4.2.1 Small samples.....	29
4.2.2 Fractured samples.....	32
4.2.3 Different test.....	33
4.3 Optical Microscopy analysis.....	33
4.3.1 Grain boundaries.....	33
4.3.2 Crack analysis.....	36
4.3.3 Fracture analysis.....	37
4.3.4 Topography differences.....	37
4.4 SEM and EDX analysis.....	38
4.4.1 Element mapping.....	38
4.4.2 Thickness gain and thickness loss.....	43
5. Discussion.....	45
5.1 Bent samples.....	45
5.2 Fracture position - tensile.....	46
5.3 Colour changes after PCM heat treatment.....	47
5.4 PCM flaking.....	48
5.5 Limitations.....	49
6. Conclusions.....	50
6.1 Future work.....	51
6.1.1 Completion of tests.....	51
6.1.2 Different conditions.....	51
6.1.3 Different mechanical tests.....	52
6.1.4 Different imaging.....	52
7. References.....	53
8. Appendices.....	60
8.1 Manuscript.....	60
8.2 Tensile stress.....	60
8.3 Vickers Hardness testing.....	63
8.4 Optical microscopy.....	70
8.5 SEM and EDX.....	74

List of Figures

Figure 1 – Diagram of the processes inside a concentrated solar thermal power plant.

Figure 2 – Microstructure of SS 316L bulk and weld material considering austenite and ferrite grain differences.

Figure 3 – Stress strain diagram of thermally affected Inconel 625 samples. Example of Portevin-Le Chatelier effect.

Figure 4 – Standard butt weld (left). Diagram of the cross section (right). Details of the welding procedure (bottom).

Figure 5 – Dogbone sample dimensions.

Figure 6 – Struers’s polishing and grinding machine.

Figure 7 – Cylindrical furnace, utilised for both argon heat treatment and PCM heat treatments (left). Example of required crucible for heat treatment of all samples (right).

Figure 8 – Furnace used for heat treatment (left). Samples during the heat treatment (right).

Figure 9 – Instron stress tester.

Figure 10 – Struers’s Vickers hardness tester.

Figure 11 – Positions of testing and affiliated position numbers. Test set one for the small samples (top). Test set two on the fractured samples (bottom).

Figure 12 – Zeiss electric optical microscope.

Figure 13 – Scanning electron microscope accompanied by energy dispersive X-ray spectroscopy.

Figure 14 - Similar welded Inconel 625 stress strain curve of three conditions.

Figure 15 - Similar welded stainless steel 316L stress strain curve of all four conditions.

Figure 16 – Stress strain curve comparing all four dissimilar weld samples.

Figure 17 – Comparison of central Vickers hardness values, for all four dissimilar weld samples. Considers the cross-sectional surface of polished small samples.

Figure 18 - Comparison of top/butt weld Vickers hardness values, for all four dissimilar weld samples. Considers the cross-sectional surface of polished small samples.

Figure 19 - Comparison of bottom/smooth weld Vickers hardness values, for all four dissimilar weld samples. Considers the cross-sectional surface of polished small samples.

Figure 20 - PCM heat treated dissimilar weld sample without polishing. Cracking of stainless steel 316L (top) and Inconel 625 (bottom) sections.

Figure 21 - Comparison of fracture positions for dissimilar weld samples. Pristine sample (left) argon heat treated (centre) and air heat treated (right).

Figure 22 – Elemental mapping of the dissimilar weld’s pristine small samples cross section, located at the stainless steel 316L to weld line.

Figure 23 – Elemental mapping of the dissimilar weld’s argon heat treated small samples cross section, located at the stainless steel 316L to weld line.

Figure 24 – Elemental mapping of the dissimilar weld’s air heat treated small samples cross section, located at the stainless steel 316L to weld line.

Figure 25 – Elemental mapping of the dissimilar weld’s PCM heat treated small samples cross section, located at the stainless steel 316L to weld line.

Figure 26 – Chart comparing the material loss at positions 1, 2, 4, 6 and 7 for all heat treatments of dissimilar weld small samples.

Figure 27 - Chart comparing the material gain at positions 1, 2, 4, 6 and 7 for all heat treatments of dissimilar weld small samples.

Figure 28 – Example of bent sample.

Figure 29 – Pristine and argon heat treated dogbone samples, before (left) and after (right) the tensile strength test.

Figure 30 - Presence of solid PCM remaining after heat treatment.

Figure 31 – PCM heat treated dogbone samples. Dissimilar weld front (left) and back (centre), accompanied with front image of stainless steel 316L similar sample (right).

Figure 32 - PCM heat treated dissimilar weld sample after fracture. Inconel 625 to weld cross section (left). Coving plate broken away from Inconel 625 (centre). Flaking of stainless steel 316L (right).

Figure 33 – Stress strain curve of PCM heat treated dissimilar weld sample, before correction was applied.

Figure 34 - Air heat treated dogbone samples both before (left) and after (right) fracture.

Figure 35 - PCM heat treated dogbone samples both before (left) and after (right) fracture.

Figure 36 - Example of size differences from the same point due to unpolished surface.

Figure 37 - Example of distortion on unpolished samples.

Figure 38 - Example of slipping in multiple situations, Polished samples (left) PCM heat treated samples (centre) Unpolished samples (right).

Figure 39 - Images of hardness points from the broken oxidised Inconel strip. 3 separate tested positions.

Figure 40 - SEM images small cross section air heat treated samples after fracture located at the weld lines. Butt of weld perspective (left) and long weld perspective (right).

Figure 41 - EDX image of oxygen content below weld line. Air heat treated cross section of small samples.

Figure 42 - EDX of dissimilar weld small sample, after air heat treatment with no polishing.

Figure 43 - EDX of stainless steel 316L similar weld small sample, after air heat treatment with no polishing.

Figure 44 - EDX of Inconel 625 similar weld small sample, after air heat treatment with no polishing.

List of Tables

Table 1 - Elemental composition of stainless steel 316L.

Table 2 - Elemental composition of Inconel 625.

Table 3 - Table of each treatment's mechanical properties for similar weld Inconel 625 samples.

Table 4 - Table of each treatment's mechanical properties for similar weld stainless steel 316L samples.

Table 5 - Table of each treatment's mechanical properties for dissimilar welded samples.

Table 6 – Average centre/position 3 hardness of welded stainless steel 316L samples after different treatments.

Table 7 – Grain boundaries for sections 1,2, 6 and 7 on all small dissimilar weld samples.

Table 8 - Dissimilar weld dogbone samples before and after fracture.

Table 9 – Average hardness of all fractured dissimilar weld samples, without polishing.

Table 10 – Hardness of dissimilar weld small samples with different treatments after polishing.

Table 11 - Hardness of similar weld stainless steel 316L small samples with different treatments after polishing.

Table 12 – Hardness of small samples air heat treated before polishing.

Table 13 – Hardness of small samples air heat treated after polishing.

Table 14 – Hardness of different polished treated dissimilar weld samples after fracture.

Table 15 – Hardness of different treated dissimilar weld samples after fracture. No polishing process applied.

Table 16 - Hardness values for different treated stainless steel 316L similar weld fractured samples. No polishing process applied.

Table 17 - Hardness values for different treated stainless steel 316L similar weld fractured samples. No polishing process applied.

Table 18 - Fractured samples hardness values where points get 1 mm closer to weld. Taken from position 2.

Table 19 - Hardness values of fractured PCM heat treated, similar weld Inconel 625 samples, underneath the broken oxidised surface.

Table 20 - Pre fracture PCM hardness values.

Table 21 – Topography of pristine dissimilar weld fractured sample, when unpolished.

Table 22 – Topography of PCM heat treated dissimilar weld fractured sample, when unpolished.

Table 23 - Differences in welds of dissimilar weld samples after different treatments of unpolished samples before and after fracture.

Table 24 - Differences in welds of dissimilar samples after different treatments of polished samples before and after fracture.

Table 25 - SEM images of polished air heat treated cross section, dissimilar weld samples after fracture.

Table 26 - Images of unpolished air heat treated dissimilar weld small samples, at different positions.

Table 27 - Images of unpolished stainless steel 316L similar weld air heat treated small samples, at different positions.

Table 28 - Material loss estimation on unpolished air heat treated small samples.

Table 29 – Material loss average values.

Table 30 – Material gain of dissimilar weld samples after each treatment, determined through EDX oxygen levels and visible differences, at the 5 main locations.

List of Calculations

Calculation 1 – Elongation/ductility

Calculation 2 – Youngs modulus

Abstract

Dissimilar welding is a common practice in industrial systems. The process allows for specific or improved mechanical and chemical properties to be applied over specific sections, allowing for specific environments to be sustainable and costs to be reduced. Concentrated solar thermal power plants are one such system, which requires stainless steel 316L and Inconel 625 to be dissimilarly weld. The differing thermal and corrosive conditions that are present at different points, require the different properties provided by each material. The process of welding is similar to applying a heat treatment and thus may alter the material. This study aims to explore if the welding process has caused a mechanical or chemical alteration in the material. Reviewed literature covers all information based on dissimilar welds between the two materials. It shows that little research has been complete when considering the eight key points, leaving a large gap in understanding. The methodology covers the welding process, reasons for applying argon, atmospheric and phase changing material (PCM) based heat treatments, procedures followed for conducting tensile stress and Vickers hardness tests. The amount and type of optical microscopy, SEM and EDX techniques utilised are also considered. The tests produced results on the ultimate tensile strength, hardness, changes in the grain boundaries, level of material loss and elemental presence. Each result was compared to literature and showed the presence of trends in both the hardness and tensile stress. From these comparisons the main results determined are that the bulk material and welded material appear to have very similar tensile strength and hardness but differ in ductility and stiffness.

DECLARATION

I certify that this thesis:

does not incorporate without acknowledgment any material previously submitted for a degree or diploma in any university

and the research within will not be submitted for any other future degree or diploma without the permission of Flinders University; and

to the best of my knowledge and belief, does not contain any material previously published or written by another person except where due reference is made in the text.

Signature of student

Print name of student: DANIEL ALEXANDER SHORE

Date: 07/10/2022



I certify that I have read this thesis. In my opinion it is/is not (please circle) fully adequate, in scope and in quality, as a thesis for the degree of Bachelor of Science (Chemical science) (Honours), Masters of Engineering (Materials). Furthermore, I confirm that I have provided feedback on this thesis and the student has implemented it minimally/partially/fully (please circle).

Signature of Principal Supervisor *Reza Hashemi*

Print name of Principal Supervisor: Reza Hashemi

Date: 17/10/2022

Acknowledgements

This report has been supported by multiple people and groups. Decisions and directions of the study were made with the supervision of Reza Hashemi and assisted by Gunther Andersson. Further direction and previous (published and unpublished) results in similar areas were provided by the ASTRI Flinders group, led by Gunther Andersson and consisting of Reza Hashemi, Alex Gressier, Yanting Yin and Cooper Nohlmans. The funding from ASTRI is also acknowledged, allowing for the materials and tests to be conducted. The assistance from Flinders microscopy and Flinders Engineering services with developing methodologies, creating samples and testing is also acknowledged.

1. Introduction

1.1 Background

Renewable energy is an important and ever-growing industry which is expanding at an ever-growing rate in all areas. Solar methods have one of the largest potentials and highest rooves for production of energy. With its predictable and constant presence throughout the year, a reliable energy return can be calculated, which is currently predicted to be capable of providing the entirety of the earths power requirements [1]. One of the current issues revolves around the integration of batteries and other energy retention methods, with them being too small and inefficient to be considered a sole power source [2]. Solar panels are the most common method and work through the conversion of light to electricity through photovoltaic cells [3]. A different more industrial method is concentrated solar thermal power plants (CSTP). This system is designed to convert solar radiation into thermal energy and then into electricity.

A typical design of CSTP consists of a series of mirrors and lenses which angles and amplifies solar radiation beams towards a thermal receiver, as seen in Figure 1. This is filled with a heat transfer fluid. This is commonly a sodium-based fluid, due to its stable and high thermal conductivity [4]. This fluid heats up as the day goes on and proceeds to transition through a series of pipes into storage tanks. Parallel water pipes to the tanks conduct the heat, producing steam which pushes turbines, allowing for a generator to convert kinetic energy into electricity.

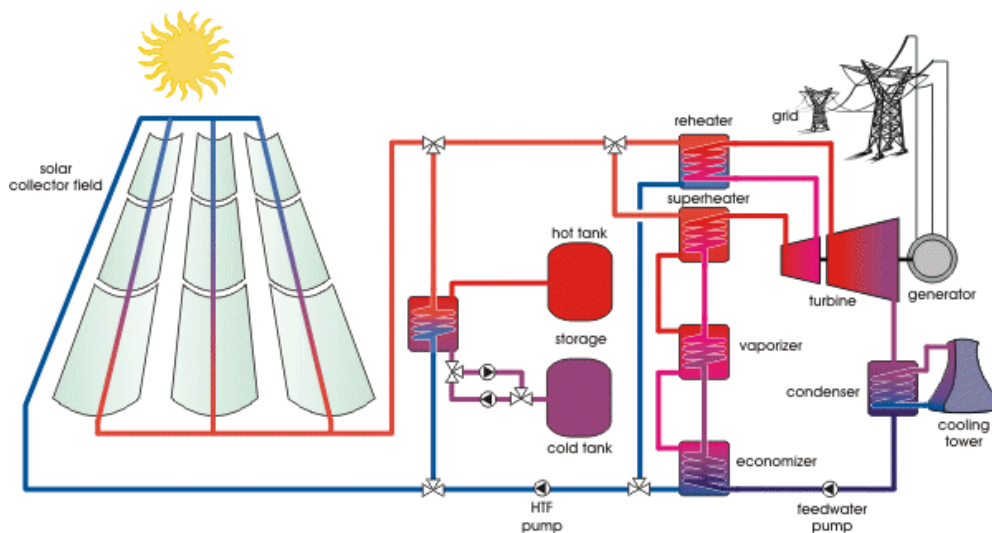


Figure 1 – Diagram of the processes inside a concentrated solar thermal power plant [5]

(Reproduced with permission).

1.2 Definition of problem

In this process of creating electricity, the CSTP system gets anywhere from 500 to 1000 degrees centigrade. These high temperatures partnered with the corrosive nature of sodium create a very hostile environment. These conditions exist throughout most of the system and therefore affect both the tubing and storage (usually box shaped) systems. Due to this, materials which are strong at prolonged high temperatures and will experience little/predicable material loss due to corrosion, are utilised. Stainless steel 316L (SS 316L) and Inconel 625 both possess these qualities. SS 316L has a reduced carbon concentration, reducing its chances of corrosion. Inconel is a nickel based super alloy giving it improved chemical resistances, better mechanical strength, and hardness as well as more consistent properties at high temperatures [6, 7]. Through comparing their elemental composition, as seen in Tables 1 and 2, with their known mechanical properties, Inconel 625 is a more desired material. However, Inconel 625 is considerably more difficult to obtain and hence more expensive, making it undesirable to use in large projects. Due to this, dissimilar welds are wanted to be employed between the SS 316L and Inconel 625. This allows for the positions under the greatest thermal and chemical stress to be constructed out of Inconel 625 and the remaining from SS 316L, thus reducing the cost but still improving the structural integrity. The issue revolves around the lack of information around whether these welding process will alter the mechanical and/or chemical properties of both the materials surrounding the weld or the weld itself.

Table 1 - Elemental composition of stainless steel 316L [6].

Component	C	Cr	Fe	Mn	Mo	Ni	P	S	Si
Weight percentage (%)	0.03	17	65	2	2.5	12	0.045	0.03	1

Table 2 - Elemental composition of Inconel 625 [8].

Component	Ni	Cr	Mo	Fe	Nb + Ta	Co	Mn	C	S	Si
Weight percentage (%)	58	21.5	9	5	3.65	1	0.5	0.1	0.01	0.5

1.2 Significance

This understanding of the welded section is very important to the CSTP systems and potentially any other industrial process which requires a hostile environment. Due to the scale of CSTP systems any way which the cost can be reduced is important to be explored. The reduction of cost increases the likelihood of the project being undertaken and complete successfully. The ability to understand how a material will react under different conditions and configurations, creates opportunities for different systems to be developed in the future.

1.3 Aims

Considering this information, this study has a clear set of aims that it will explore.

1. Test the mechanical properties of welded stainless steel 316L and Inconel 625 samples both in a similar and dissimilar configuration.
2. Test and compare the samples in different environments to determine if and how the mechanical properties are affected.
3. Test and compare the samples in different environments and consider what chemical effects have occurred and why.

By considering these points a comprehensive understanding of the subject shall be obtained and create a platform for future work to be complete.

To complete these aims multiple steps will be complete. Each step has been split into a separate chapter starting with a literature review. In this stage the current literature revolving around the mechanical and chemical properties of the materials as well as information on weld preparation and effects. Using this information, the next chapter will state the methodology followed including the acquiring and preparation of samples, followed by the testing and characterisation methods. From here the results will be considered in a series of tables, graphs and illustrations. These shall be accompanied by a concise explanation giving the surface level understanding. The discussion will consider literature and other sources to explain the less obvious aspects of the results. The final chapter shall conclude the study by reiterating if the aims where met and what future research can be considered due to this study.

2. Literature review

As stated in the introduction, this report will be considering the effects which dissimilar welds may cause to mechanical and chemical integrity of the material. A series of key points which must be considered are; Inconel 625, stainless steel 316L, dissimilar welds, plates/liner geometry, thermal conditions, corrosive conditions, mechanical behaviours and chemical behaviours. To successfully complete a review of the current literature, all aspects of these eight key points must be considered both individually and collectively. Initially the history must be considered to understand what has already been established. These understanding can then be combined and considered simultaneously to find the most relevant literature, therefore exposing any gaps.

2.1 Individual points

Firstly, the materials were considered. The easiest way to complete this was to research through material databases such as AZOM, MatWeb, E-Z LOK database and World Materials, for both SS 316L and Inconel 625. Basic information such as element composition, basic mechanical qualities and their greatest strengths can be determined through these types of databases. Through quick research, multiple websites ranging from blogs to research studies were found on the topic [9, 10, 11]. Stress strain curves were seen to be the most commonly test preformed, as many properties could be determined. The ultimate tensile strength and Young's modulus were the two most covered due to there more consistent and obtainable nature. In some of the more particular studies the hardness values were also deemed very important due to the ease in repeating the test or simultaneously considering multiple points on the same sample [12, 13]. Considering this, these properties as found on the databases are as follows. For SS 316L, properties of 485 MPa tensile strength, 193 GPa Young's modulus and 152 Vickers hardness [14, 15, 16, 17]. Inconel 625 has the greater properties of 827 MPa tensile strength, 205 GPa Young's modulus and Vickers hardness of 253 [18, 19, 20, 21]. The elemental percentages were also listed in these databases.

For the configurations, research into dissimilar welding was focused upon. It was discovered through authors such as D. I. Roberts [22] and A. Joseph [23], who wrote studies on dissimilar welds, that for 40 plus years there have a plethora of industrial applications. Since 1991 multiple articles show more consistent and dedicated methods of preforming this type of welding. Information such as “*similar elongation to the bulk material*”, “*preheating is*

required to reduce cracking” and *“oxygen layers commonly form around the dissimilar weld”* were commonly mentioned [24]. Decades later multiple welding directories which give methods of reducing thermal expansion, decreasing staining and the chance of oxidation layers forming are discussed [25]. Multiple scientific studies also compare different proposed welding methods with varying degrees of specificity [26]. Dissimilar welds containing vastly different bulk materials i.e., an iron based material to an aluminium or nickel, was very uncommonly spoken about. Any articles considering these points usually consider the weld as a different material to a single bulk material.

Finally, for the conditions, possible thermal levels in CSTP systems were further researched into, to determine what temperature ranges are present. The CSIRO stated that constant temperature of 590 degrees centigrade were obtained in 2013 [27], whilst The Australian Academy of Science claim temperature up to 1000 degrees centigrade can be reached [28]. Considering this, a temperature of 750 degrees would be a good middle ground to test both high level application and long time periods under stress.

Conditions of high corrosion were researched through a wide variety of studies on a multitude of metals. The studies undertaken by D. Mei [29] and F.L Laque [30] gave an understanding of the required processes to measurable corrosion levels. The articles stated that the chemical conditions must be understood and then each element must be isolated, such that the affect a level of corrosion can be determined. Simultaneous exposure could then be compared to understand if further mechanisms are present. This methodology of testing could be applied in this study.

2.2 Most relevant research

From here, more relevant studies were considered. These studies initially had to consider any form of weld with at least one of SS 316L and Inconel 625, as the bulk materials. 40 – 50 articles with some relevance were discovered. SS 316L based studies mainly considered corrosion affects, welding technique affects and some information on microstructures and mechanical properties.

A. Moteshakker [31], H. Liqing [32], M. Dadfar [33] and C. Ma [34] all researched into corrosion affects. This ranged from corrosion caused by the welds, resistances, and corrosion levels after pure heating processes. All these studies exclusively characterise the similar or dissimilar weld through selective electron microscopy (SEM), X-Ray powder diffraction

(XRD) and electron-dispersive X-ray spectroscopy (EDS). Many of these articles also considered tungsten inert gas (TIG) welding methods due to the extra control and lower chances of warping effects on small samples. Other articles [34, 35] specifically considered the microstructures. The most interesting point from these studies considered the presence of austenite and ferrite grain boundaries, with examples of their presence in both bulk material and welds. A final series of articles compared similar and dissimilar weld properties [36, 37]. These articles also characterised the microstructure showing effects of different grain boundaries and directions. Properties such as the yield and tensile strength, ductility, and hardness were measured and considered to represent the same properties as the bulk material.

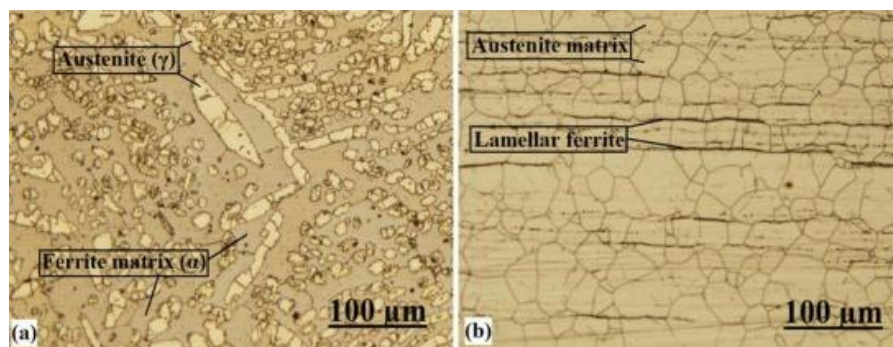


Figure 2 – Microstructure of SS 316L bulk and weld material considering austenite and ferrite grain differences (Reproduced with permission).

Inconel 625 based studies were a little less in depth and more commonly considered similarly welded samples. The first articles written by H. Vemanaboina and J. Sivakumar considered mechanical and metallurgical properties [38, 39]. Multiple welding methods were considered and analysed with different tests being applied to each. TIG weld samples focused on characterisation through XRD and different thermal based analysis methods. A more particular article, written by P. Corigliano, focused on the fatigue of dissimilar welds and concluded that good weld levels could still be obtained [40]. M.M.D Oliveria studied a more generalised aspects based on the thermal effects of Inconel 625 [41], whilst focusing on tensile strength and creep testing. The most important point stated, was that Inconel 625 is affected by the Portevin-Le Chatelier effect. This is where an unstable plastic deformation flow occurs, creating jagged lines in stress strain curves. The article tested different rates showing that slower ones increased the affect. Other articles were consulted showing stress rates of 1 – 10 mm/min where considered, creating successful results. A final article

consolidated much of the research mentioned previously and related it to corrosion properties.

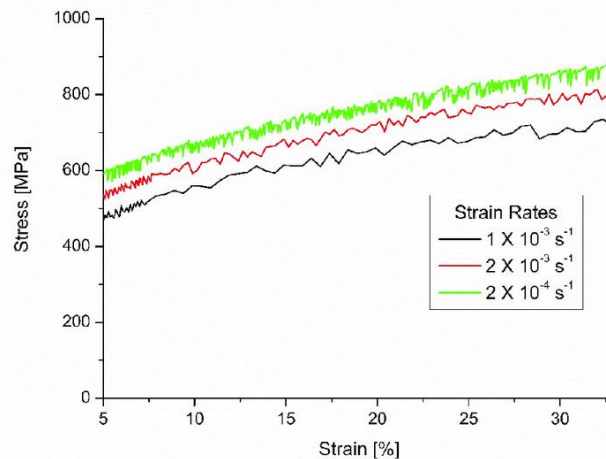


Figure 3 – Stress strain diagram of thermally affected Inconel 625 samples. Example of Portevin-Le Chatelier effect [41] (Reproduced with permission).

The final aspect of research solely considered dissimilar welds between the two materials. The three articles found were written by A. Kulkarni [43] K. Kumar [44] and T. Ramkumar [45]. A form of tungsten weld was always considered in these articles. All three looked at the tensile strength and hardness accompanied by microstructural analysis. Bending and impact toughness were also considered. The most important points deduced that Inconel 625 tensile properties were reduced, the fracture always occurred in SS 316L samples and dissimilar welds possessed greater hardness. None of these articles considered thermal or chemical affects.

After considering all these articles it could be seen that, there was no article discovered which covered all eight key points in the same report. There is multiple which cover five to seven, with one point from each of the baseline areas.

2.3 Gap in literature

It can now clearly be seen that there is a gap in this literature. The provided literature has shown to cover all aspects of the eight key points as individual aspects. Many different pieces of literature showed the direction of each key point, but very little considered more than 6 of the points simultaneously. The key point of dissimilar welds, was the hardest point to find information on. Greater than 80% of the found literature referred to dissimilar welds between

similar materials, ie; Inconel 625 to Inconel 718, therefore not covering as larger spectrum as this report aims to. Due to this it can be said there is a gap in literature, relating to mechanical properties of dissimilar welds between stainless steel 316L and Inconel 625 for high temperature corrosive applications.

3. Methodology

There are a multitude of mechanical and chemical tests which can be complete under a multitude of different conditions. Due to the read literature, it was decided to consider three different mechanical tests for three different sample configurations, which will have four different treatments applied. Different levels of analysis will then be applied to each tested sample, depending on the results of the mechanical testing. This will be complete on a set of linear samples.

3.1 Sample preparation

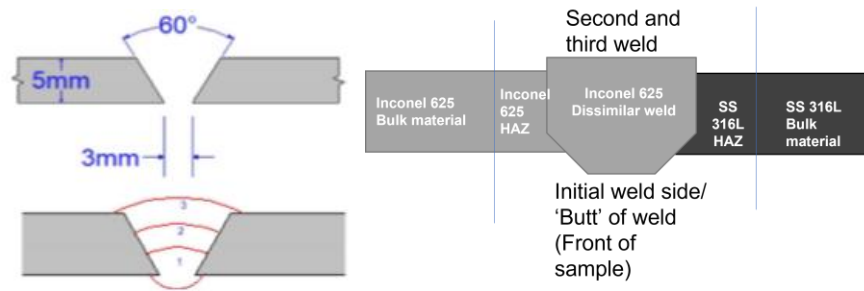
As stated there will be three different configurations which are;

1. Inconel 625 welded to Inconel 625, with an Inconel 625 filler material (similar Inconel).
2. SS 316L welded to SS 316L, with a SS 316L filler material (similar SS).
3. Inconel 625 welded to SS 316L, with an Inconel 625 filler material (dissimilar).

Each configuration will be welded and cut in the same manner to maintain consistency and create the greatest accuracy possible.

3.1.1 Welding process

A tungsten gas arc welding method with a forehand technique was used for all welded samples. The two plates with dimensions of 300 mm * 92 mm * 5 mm (L*W*D), would create a butt weld as seen in Figure 4. A single running is applied to make a short section, which is defined as the 'butt' (for this study the top position), whilst multiple passings are applied to the opposing side, making a longer and thinner weld section. 6 to 8 mm beside this weld on both sides is considered the heat affected zones (HAZ). This material will potentially have slightly different mechanical properties. This process was completed by Technoweld (located in Adelaide) [46]. This welding process followed AS/NZS 3992-2020 standards [47].



Joint Tolerances		Diameter – Thickness		Thermal treatment	
Bevel Angle:	60°Inc.	Pipe Diameter:	n/a	Preheat °C:	42°C
Root Gap:	3mm	Thickness Range:	n/a	Inter-pass °C:	90°C
Root Face:	0mm	Combined Thickness:	10mm	P.W.H.T.:	n/a
Consumable Details and Welding Parameters					
Consumable Classification:	ER NiCrMo3	Technique:	Fore Hand / Push		
Trade Name:	Metrode	Electrode Stickout:	15mm		
Batch No:	WO80172	Metal Transfer:	n/a		
Tungsten Type/Size:	Thoriated 2.4mm	Purge Gas / Flow Rate:	10Lpm.		
Shielding Gas:	Argon	Interrun Cleaning:	Wire Brush		
Flow Rate:	15Lpm.	Flux Class / Batch:	n/a		

Figure 4 – Standard butt weld (left). Diagram of the cross section (right). Details of the welding procedure (bottom) [48] (Reproduced with permission).

3.1.2 Cutting processes

After the welds were complete, multiple samples were cut. Four dogbone and four small samples were cut from each of the three configurations. Figure 5 shows the dimensions used for the dogbone samples. The small samples were cut to be around 20 mm * 10 mm * 5 mm. All cutting procedures utilise an IsoMet saw and were completed by Engineering services, located in the Tonsley campus of Flinders University. The IsoMet saw was used to reduce the possibility of creating weaker points via the creation of cracks or excessive localised heating [49].

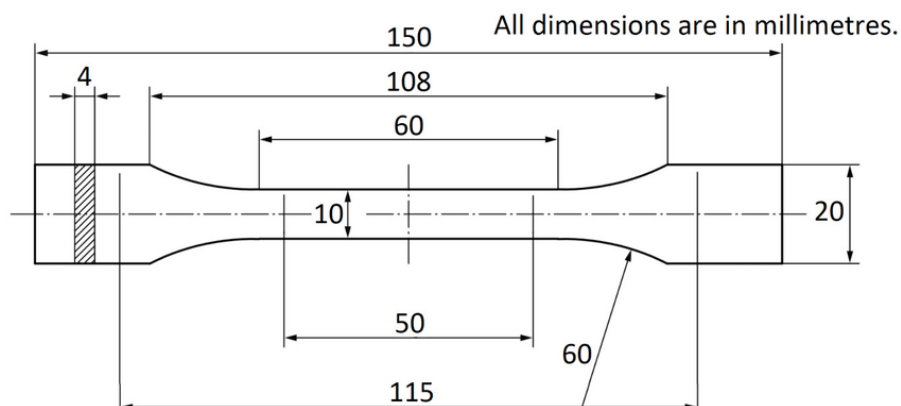


Figure 5 – Dogbone sample dimensions [50], (Reproduced with permission)

After testing is completed, fractured samples were cut to both separate the fracture zone from the bulk material, allowing for both a fractured sample cross section and fracture zone to undergo characterisation processes.

3.1.3 Polishing process

The small samples and fractured dogbone cross section samples, after they have been cut to their cross section sizes, were polished. This step is required to increase the visibility for characterisation processes and accuracy of mechanical tests. A process of polishing and grinding was complete at Flinders University, Tonsley campus in the mechanical testing room on the Struers's polishing and grinding machine. Each sample was individually set in one of the "Struers's selection guide" plastics, depending on the samples size. A four-step process which is based off the "Struers's metallographic preparation of stainless steel" was undertaken [51]. Step one flattens the surface using a low grit silicon carbide paper, whilst steps two and three reduce the scratch size and the final step applies the polish.



Figure 6 – Struers's polishing and grinding machine.

3.2 Testing details

For each of the three different sample configurations, four different conditions will be considered. These are; pristine, argon heat treated, air heat treated and phase changing material (PCM) heat treated. As stated in the literature review, each of these conditions were considered to some regard, however every one of them was not considered simultaneously in the same report or article. All these treatments are applied after the samples have been cut (dogbones and small samples).

3.2.1 Pristine

Pristine conditions refer to no heating or chemical treatments being applied after the welding process.

3.2.2 Argon heat treated

This treatment process is conducted in a split tube furnace (STF) with a cylindrical design, as seen in Figure 7. In this process a constant air flow accompanied by an oxygen bubbler is applied to create a flow direction, removing reacting gases and creating a pressure increase to improve the temperature consistency. In this treatment an argon flow of greater than 2 ppm is applied, for 500 hours at 750 degrees centigrade. This temperature was chosen as it is deemed an accurate representation of the average temperature present in CSTP the systems. The argon flow is designed to remove all atmospheric conditions created by an outside source, therefore allowing for only thermal conditions to be tested. The crucible, which can be seen in Figure 7, further reduces the chances of the atmosphere in producing chemical reactions.

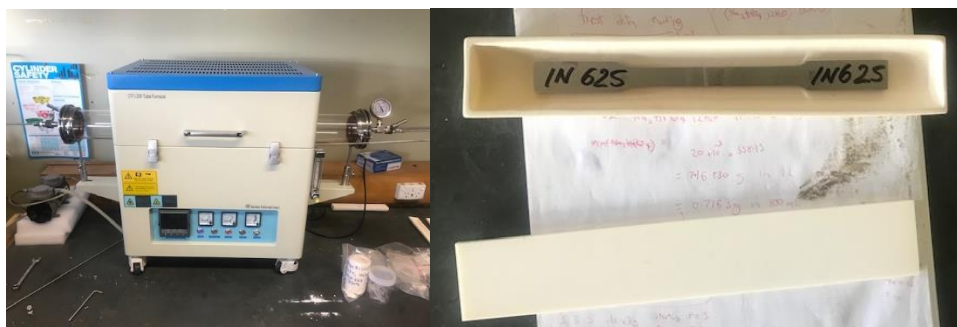


Figure 7 – Cylindrical furnace, utilised for both argon heat treatment and PCM heat treatments (left). Example of required crucible for heat treatment of all samples (right).

3.2.3 Air heat treated

The air heat treatment is complete in a standard furnace, which was located at the Flinders University, Bedford Park engineering services workshop. This test went for 500 hours at 750 degrees centigrade, keeping the test consistent with the argon heat treatment. This test is designed to simulate how the atmosphere or low chemical disturbances will affect the materials. As seen in Figure 8, crucibles were placed underneath the samples to increase the number of exposed surfaces. Little literature considered this type of treatment.

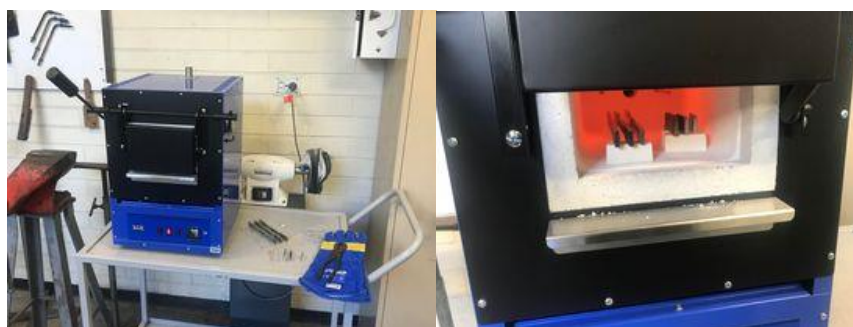


Figure 8 – Furnace used for heat treatment (left). Samples during the heat treatment (right).

3.2.4 Phase changing material (PCM) heat treated

This treatment took place in the same conditions as the argon heat treatment. The sole difference is the application of PCM in the crucible. This consists of a 45% sodium carbonate to 55% potassium carbonate salt. This test is designed to apply the greatest corrosion effects which the materials will experience inside the CSTP system, at the average thermal stresses.

3.3 Mechanical testing

It was decided to follow and repeat the most common mechanical testing procedures present in the literature. Tensile stress testing and Vickers hardness testing give a good preview of mechanical properties, which are very well documented for almost all materials. This will give a good point of comparison to determine what affects the treatments and configurations are producing.

3.3.1 Tensile stress testing

This test was complete at the Flinders University Tonsley campus, in the mechanical testing room. The Instron stress tester was utilised and accompanied by the extensometer. An official 50 kN load cell for the machinery was used, such as to apply enough force to fracture the Inconel 625 samples. A 4 mm/min extension rate was applied. Literature which performed this test on both SS 316L, and Inconel 625 samples utilised rates from 1 – 10 mm/min, with 4 mm/min being a good middle ground, which got a good level of accuracy whilst not taking too long to complete. From this test the ultimate tensile strength, elongation through both software and manual measurements, plus Youngs modulus are determined. This test was completed once for each sample configuration and condition creating 12 experiments.



Figure 9 – Instron stress tester.

3.3.2 Vickers hardness test

For hardness values all tests were complete at the Flinders University Tonsley campus, in the mechanical testing room on the Struers's Vickers hardness tester. A hardness value of 1 was used for all samples and a minimum 1 mm gap between each test was applied. This gap is designed to stop the chance of hardness values being affected by the deformation created by another test [52]. A magnification setting of 20 times was used for SS 316L samples and 40 times for Inconel 625 samples. This is due to Inconel 625 in literature having a greater Vickers hardness value, therefore producing smaller indentations. The outcome from this test is to determine what differences in hardness are present after each treatment and if there is a difference between the bulk material and weld.



Figure 10 – Struers's Vickers hardness tester.

There are 3 different tests which were complete. First was on the small polished samples. As seen in Figure 11, each of the seven different positions, where 1 represents Inconel 625 and 7 represents SS 316L (in the dissimilar weld samples), will be tested at five different levels, with the first test being closest to the butt of the weld. After the dogbones have been fractured, this will be repeated for positions 1, 2, 4, 6 and 7 for the first three tests (closest to butt weld and next two positions). Finally positions 2, 3, 4, 5 and 6 will be tested 5 times on a cross section samples of all fractured samples. Considering all these conditions, 900 hardness values will be measured, tabulated, and compared to find trends in the results.

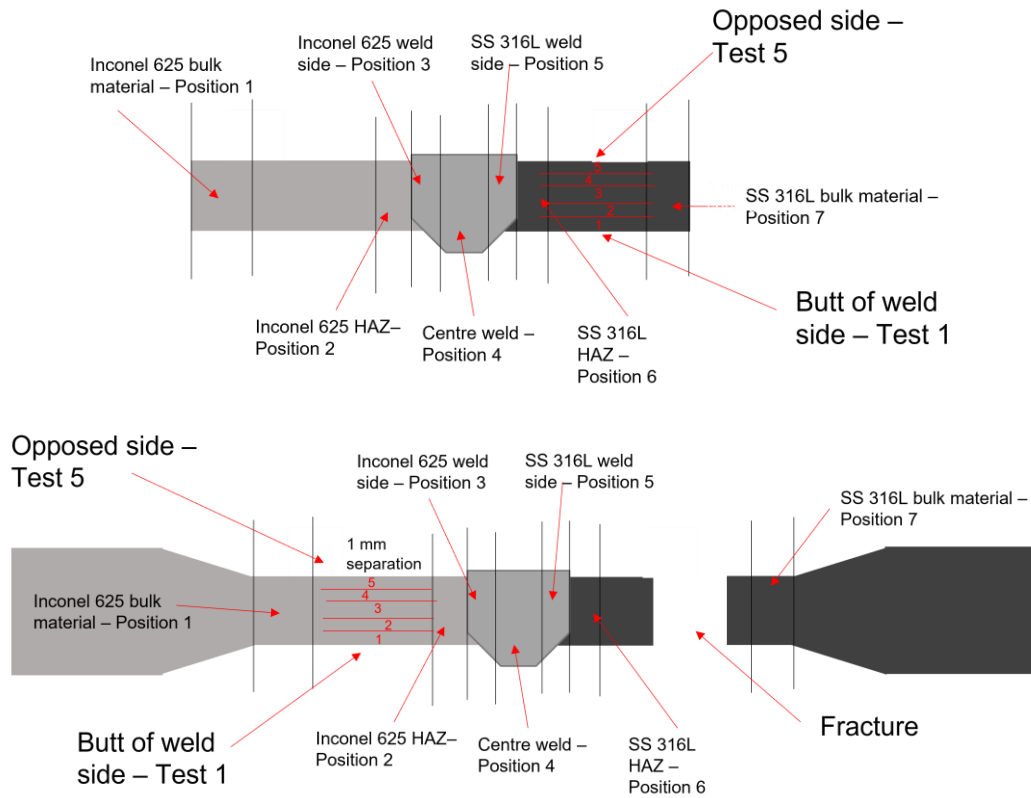


Figure 11 – Positions of testing and affiliated position numbers. Test set on for the small samples (top). Test set two on the fractured samples (bottom).

3.4 Characterisation

3.4.1 Optical microscopy

This characterisation method utilised an electric optical microscope, with the Zeiss program. Varying levels of magnification ranging from 5 times to 40 times will be used for different applications. Before the mechanical tests are complete, images were taken at positions 1, 2, 4, 6 and 7 (highlighted in hardness testing). After each test the same procedure was followed. This was to check for any changes or abnormalities in the samples which may influence the accuracy of the results. Simultaneously, the grain boundaries were analysed for each sample configuration and applied treatments. The size and number of grains are to be compared to literature and other samples. The fractured samples are also to be considered. The fractured section will be imaged and compared to literature, such as to determine further mechanical behaviours.



Figure 12 – Zeiss electric optical microscope.

3.4.2 SEM and EDX analysis

This characterisation method was complete at the Bedford Park campus of Flinders University, in the SEM/EDX laboratory. Polished small and cross-section samples of each configuration and treatment will undergo analysis. Images from all 7 position at both the centre (looking for abnormalities and consistencies) and edges (looking for colour changes to determine material loss) are to be considered for SEM analysis, with an analysis method of secondary electrons and magnification of 10 000 times. EDX images using backscattering at a magnification of 800 times, will consider the top (butt weld) and bottom welds of each sample. Elemental maps will be generated and used to determine corrosion levels and positions of transition. 216 separate images will be collected over the two methods to create a complete analysis.



Figure 13 – Scanning electron microscope accompanied by energy dispersive X-ray spectroscopy.

4. Results

Below are a mixture of graphs, tables and diagram which represent the results from this study. These results mainly refer to the dissimilar weld samples, as they are the focus of the report. Other results and interesting points can be found in the appendix, sections 8.2 through to 8.5.

4.1 Tensile mechanical properties

The tensile stress test was complete on 11 dogbone samples. The results from the tests have been grouped into each configuration, allowing for each applied treatment to be compared. Tables were constructed to show the key features of ultimate tensile stress, ductility and Young's modulus. The ultimate tensile strength was taken directly from the results and is defined as the stress required to fracture. The elongation or ductility was calculated by both the machinery and manually by marking a 50 mm gauge length (L_o) and comparing it to the length after the test (L_f). The difference became the elongation. This value could be compared to the sample length for the machine calculated, or initial gauge length for manual, to obtain a percentage value. Young's modulus was calculated by taking the gradient in the plastic zone. To retain consistency a difference of 100 MPa was considered, with the lower value being between 50 – 80 MPa. The basic calculations can be found in the appendix (section 8.2).

Figure 14 considers the Inconel 625 similar weld samples (PCM test was not complete). As can be seen, the pristine sample possessed a lower ultimate tensile strength but considerably greater ductility. The argon heat treated sample and air heat treated sample possess very similar values for all properties. Comparing the pristine values to literature, both the tensile strength and stiffness of the sample are considerably lower (827 MPa and 205 GPa respectively) [18]. The resulting average ductility does fall within the recognised values of 25-30% [53] as stated in literature. The Portevin-Le Chatelier effect, which was illustrated in Figure 3, did not appear to be present in any of the samples [41]. The slight jagged nature which is observed in Figure 14, is not present in SS 316L samples as well, which literature agrees should not occur.

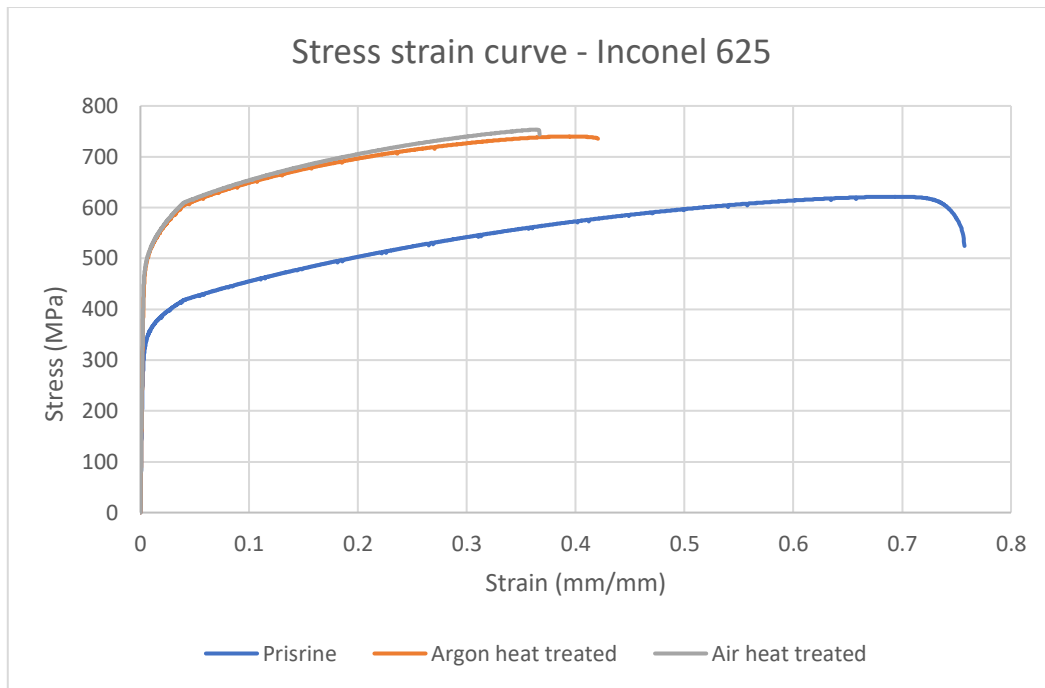


Figure 14 - Similar welded Inconel 625 stress strain curve of three conditions.

Table 3 - Table of each treatment's mechanical properties for similar weld Inconel 625 samples.

Treatment	Ultimate tensile strength (MPa)	Ductility, Instron (mm)	Ductility, manual (mm)	Youngs modulus (GPa)
Pristine	621.5	40.7 (22%)	23 (46%)	129.8
Argon heat treatment	740.1	24.7 (13%)	8.5 (17%)	160.5
In air heat treatment	753.6	23.5 (13%)	10.5 (21%)	171.2

Figure 15 and Table 4 consider SS 316L similar weld samples. The pristine sample has a lower tensile strength than the argon and air heat treated samples, following the same trend as Inconel 625. The PCM sample opposes this. Ductility also follows the same trend as Inconel 625 samples, with heat treatments decreasing the ductility drastically and PCM having the lowest. Youngs modulus differs with a decrease for both argon and air heat treated samples, but an increase for PCM samples. The pristine sample has a very similar tensile strength to literature (485 MPa) [18], lower Young's modulus and the average ductility does fall within the recognised value of 30-40% [16] as stated by literature.

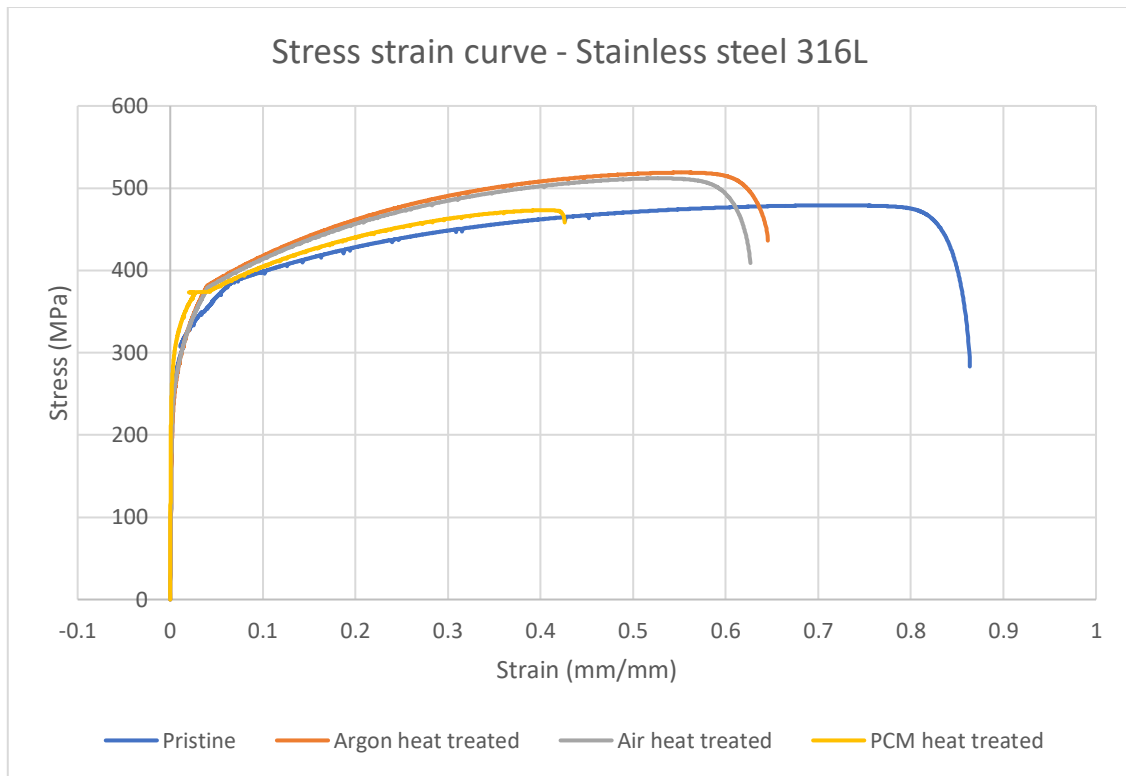


Figure 15 - Similar welded stainless steel 316L stress strain curve of all four conditions.

Table 4 - Table of each treatment’s mechanical properties for similar weld stainless steel 316L samples.

Treatment	Ultimate tensile strength (MPa)	Ductility, Instron (mm)	Ductility, manual (mm)	Youngs modulus (GPa)
Pristine	479.1	49.3 (27%)	29.5 (59%)	131.8
Argon heat treatment	519.0	36.1 (20%)	19.5 (39%)	111.1
In air heat treatment	512.0	36.3 (20%)	17.5 (35%)	126.7
PCM heat treatment	473.3	26.5 (14%)	14 (28%)	150.9

The dissimilar weld sample results are seen in Figure 16 and Table 5. These results follow the same tensile strength and ductility trends as both the similar weld samples, whilst the Youngs modulus follows the Inconel 625 samples. The pristine sample is very similar to the tensile strength and ductility values of SS 316L, therefore being similar to the literature values as well. The Youngs modulus however is considerably less.

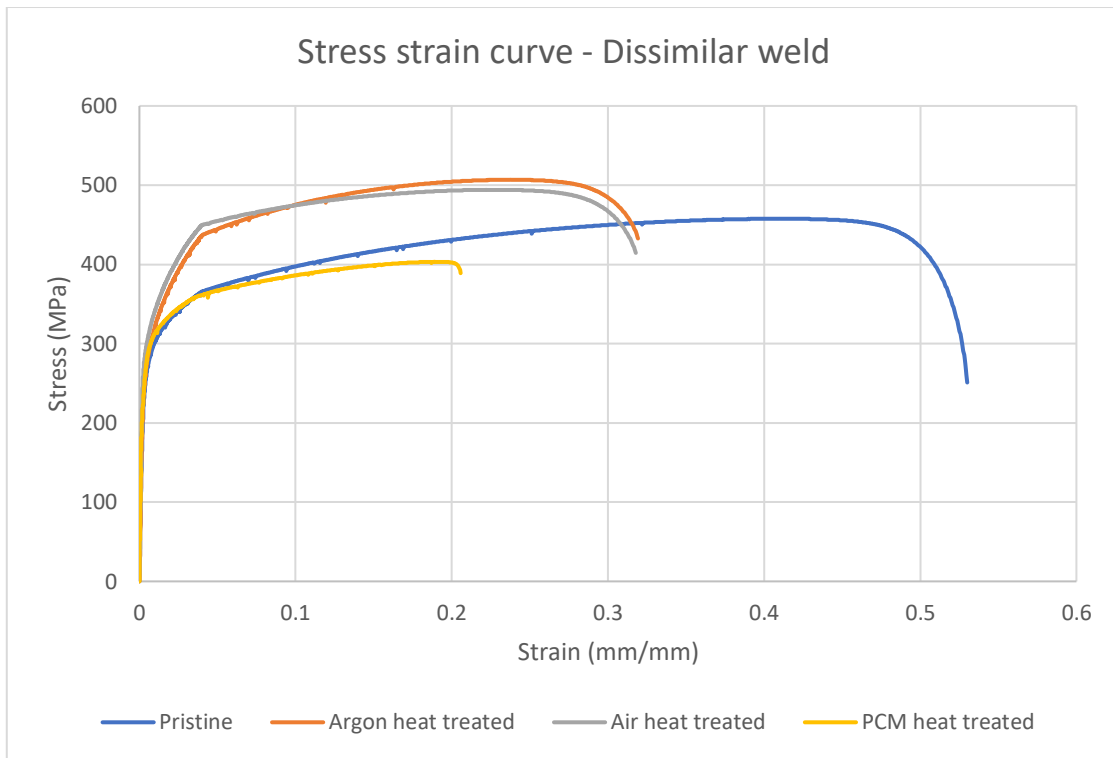


Figure 16 – Stress strain curve comparing all four dissimilar weld samples.

Table 5 - Table of each treatment's mechanical properties for dissimilar welded samples.

Treatment	Ultimate tensile strength (MPa)	Ductility, Instron (mm)	Ductility, manual (mm)	Youngs modulus (GPa)
Pristine	479.1	49.3 (26%)	16 (32%)	91.6
Argon heat treatment	506.4	20.7 (11%)	6.5 (13%)	109.7
In air heat treatment	494.2	22.8 (12%)	7.5 (15%)	143.4
PCM heat treatment	403.4	16.6 (9%)	6.5 (13%)	122.2

The PCM dissimilar weld sample must be considered with caution. During the testing, the sample had plates break away from the Inconel 625 section. This caused the clamps to slip and reduce the strain present on the sample. To compensate for this, the data was altered. The decreasing values where replaced, beginning from the last value which increased, and set to increase at the same rate as the previous 6 values. This alteration reduces the accuracy of the values but should still represent the trends accurately. The original result can be seen in Figure 33.

When observing the samples after fracture multiple comparisons to the results can be made. As can be seen in Figures 29, 36 and 37 different levels of necking are present for each sample. The level of necking correlates closely to the ductility. Less ductile samples had little necking. When considering the dissimilar weld samples specifically, as seen in Table 8, little to no change occurs in the Inconel bulk material and extreme necking occurs in the SS 316L. Thermal affects appear to be relatively consistent throughout the results, with tensile strength and Young's modulus being increased whilst ductility is decreased. This follows what most literature states [42]. Chemical affects seem to decrease the tensile strength and ductility, whilst increasing the Young's modulus. Complete literature also appears to agree with the trend of these results [54]. The biggest difference is the considerably lower Young's modulus compared to literature values. As this is present in all values, it may indicate that the weld affects the stiffness.

4.2 Vickers hardness

For these sets of results small polished dissimilar weld samples are mainly considered.

4.2.1 Small samples

The hardness values were considered in three separate sections, as can be seen in Figures 17, 18 and 19. In the centre of the cross section, all treated samples have greater hardness than the pristine sample, if point 7 (bulk SS 316L) is excluded. All samples appear to have a gradual decrease in hardness as the values transitioned from point 1 to 7. The weld portion (points 3, 4 and 5) appears to have a gradual decrease with the pristine and air heat treated samples dropping well below the literature's hardness value. The pristine sample in the bulk material (points 1 and 7) is very close to the literature values.

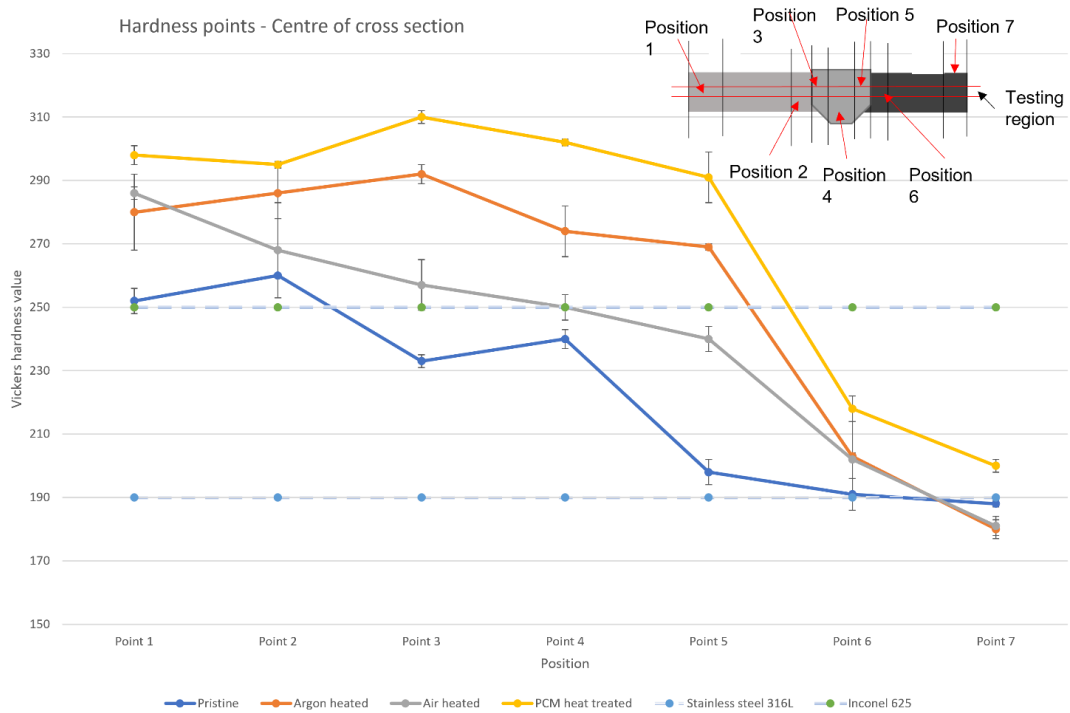


Figure 17 – Comparison of central Vickers hardness values, for all four dissimilar weld samples. Considers the cross-sectional surface of polished small samples [55].

The hardness closest to the ‘butt weld’ (test set 1) only considered points 3 to 6. Argon and PCM heat treated samples followed a similar trend, but possessed greater hardness values when heading towards position 1. When considering Table 10, it appears that air heat treated samples look to sit similarly to those in Figure 17. The pristine sample holds the largest difference, with most positions being 20 HV greater than the central values.

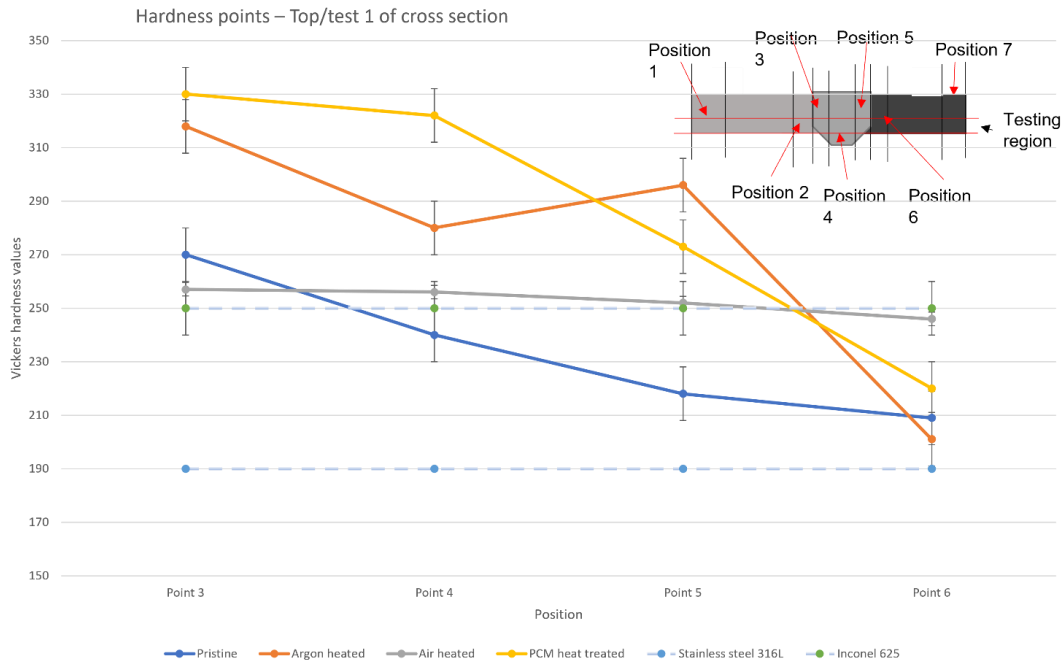


Figure 18 - Comparison of top/butt weld Vickers hardness values, for all four dissimilar weld samples. Considers the cross-sectional surface of polished small samples [55].

Figure 19 shows a much more erratic set of points. PCM and Argon heat treated samples, in general, still possess greater hardness with these values being greater than those found in the centre. The pristine sample has a very similar set of values to that found in Figure 18, being greater than those in Figure 17. The air heat treated samples however are all significantly lower.

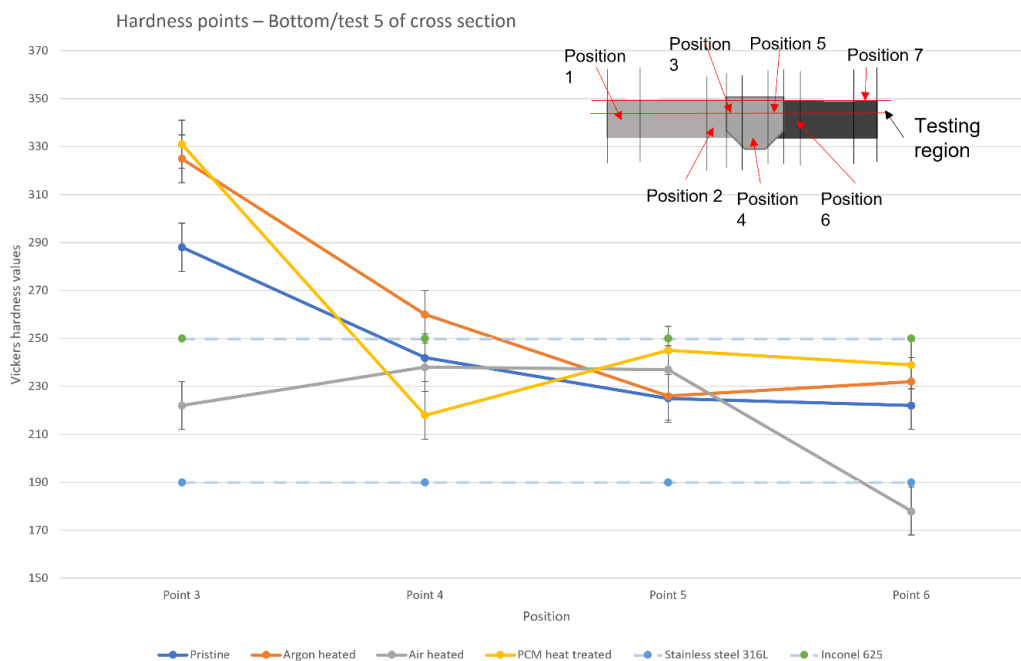


Figure 19 - Comparison of bottom/smooth weld Vickers hardness values, for all four dissimilar weld samples. Considers the cross-sectional surface of polished small samples [55].

Considering this information, it appears that the central hardness values are lower than the values taken from the edges. Neither edge looks to be consistently greater than the other. All conditions appear to slowly transition from the greater Inconel 625 hardness down into the SS 316L hardness. It is also noticed that the argon and PCM heat treating consistently increases the hardness of the bulk Inconel 625, inconsistently for the weld and not affect the bulk SS 316L too much at all. Air heat treatments also appear to have very little difference to pristine hardness samples.

When comparing these values and trends to those of similar weld SS 316L samples, as seen in Table 6, positions 6 and 7 are almost identical. Positions 4 and 5 however are much lower in Table 6. This was expected as the similar weld SS 316L samples contains a SS 316L weldment. The same trends were present with argon and PCM samples being slightly greater than the air heat treated and pristine samples.

Table 6 – Average centre/position 3 hardness of welded stainless steel 316L samples after different treatments.

Treatment type	Position 7 hardness (HV)	Position 6 hardness (HV)	Position 5 hardness (HV)	Position 4 hardness (HV)
Pristine	188	198	194	183
Argon heated	192	183	200	212
Heated in air	177	184	200	194
PCM heat treated	183	212	213	201

4.2.2 Fractured samples

The unpolished fractured sample results were tabulated and can be seen in Tables 15, 16 and 17, where dissimilar weld, SS 316L similar weld and Inconel 625 similar weld samples are considered respectively. The values produced by these tests are considerably different and are dissimilar to the literature values. However, some of the trends do appear to be consistent. Pristine and air heat treated samples are relatively similar and argon heat treated samples are slightly greater. The central values also look to be slightly lower than the exterior values. The PCM samples do not look to follow any trend and are considerably lower than the other

values. This is due to the surface of these samples being inconsistent, as the surfaces are not polished. This is illustrated in Tables 23 and 24.

4.2.3 Different test

As can be seen in Table 18, located in the appendix (section 8.3), a finer test was performed at position 2 on dissimilar weld samples. The hardness was tested at 1 mm increments getting closer to the weld. The results did not appear to demonstrate a clear pattern. This indicates that the hardness of the bulk material and heat affected zone (HAZ) is not drastically different.

As stated previously, the dissimilar weld PCM dogbone samples had plates fall from the Inconel 625 portion of the sample, during tensile stress testing. The hardness underneath these plates was tested and results can be seen in Table 19. When comparing these values to Table 15 (dissimilar weld unpolished samples) the hardness values are considerably larger underneath this top layer. When comparing them to Table 10 (dissimilar weld polished small samples) they are also much greater than the polished samples. This could indicate that only the surface after PCM heat treatment has similar properties to a pristine sample or could be an error due to the unpolished nature. Further testing would be required to confirm this.

4.3 Optical Microscopy analysis

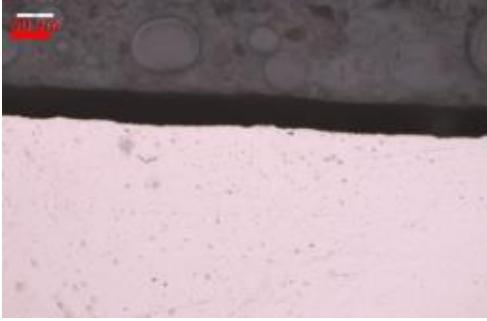
4.3.1 Grain boundaries

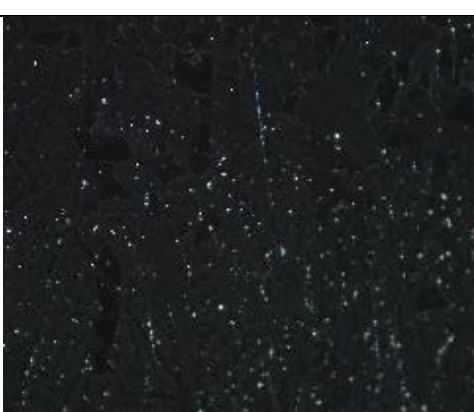
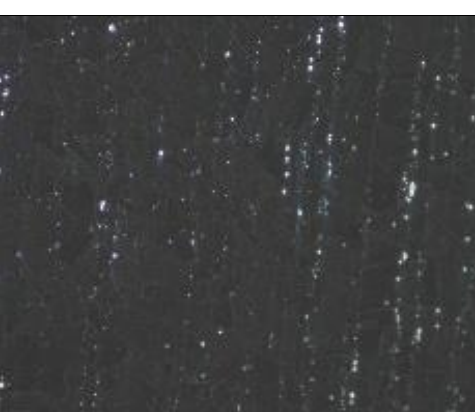
Optical microscopy analysis was complete over multiple positions of all samples, as stated in the methodology. The grain boundaries located at positions 1, 2, 6 and 7 are some of these points. Table 7 considers the dissimilar weld small, polished samples, in all 4 conditions. As can be seen, the grain sizes and number of grains present at each position, looks to be relatively consistent between all positions and samples. The grains have a varying size from 20 – 60 μm in length and 15 – 40 μm in width. Most grains look to make a rough four sided shape, with a couple others being five or six sided. When considering literature about grain boundaries [56], they are stated to be from 1 μm to 1 mm in diameter. It is stated that small grain boundaries increase the strength and hardness of a material. Literature states that if the average grain size is less than ten times smaller than the samples smallest dimension, then the sample usually has high strength and hardness values [57]. The grain size for all samples falls under this category. This makes sense as the tensile strength and hardness values produced as well as literatures understanding, indicate the same behaviour.

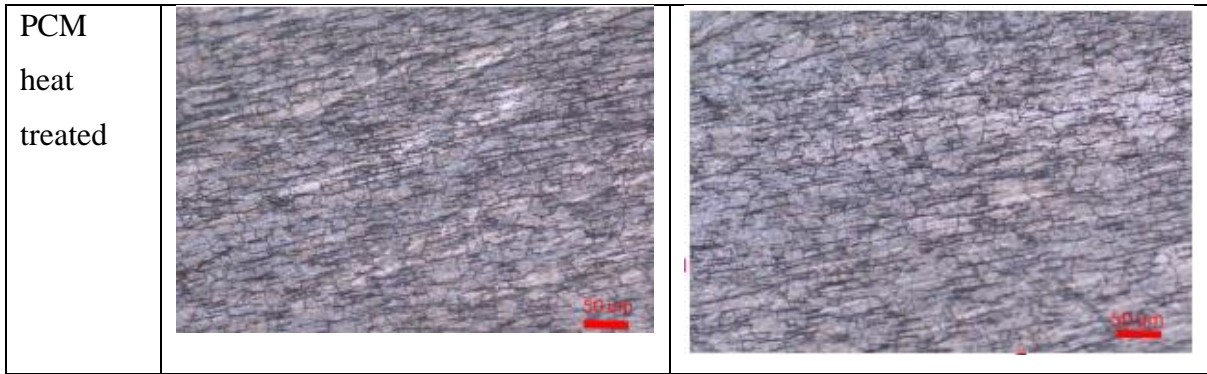
Table 24 (section 8.4) shows the welded sections before and after fracture. The grain boundaries are much harder to distinguish in this area. Something which was noted, is that the grain boundaries do appear much larger in the fractured samples. As the process of fracturing is stretching the sample, this makes sense, however literature did not appear to cover this making speculation difficult.

Treated samples at positions 6 and 7 have a series of lines which run through the grains. These are most likely ferrite lines. The literature review [34, 35] found that this commonly occurs in SS 316L treated samples and is generally deemed a hinderance due to the magnetic tendencies. This could represent part of the wors qualities present in PCM samples.

Table 7 – Grain boundaries for sections 1,2, 6 and 7 on all small dissimilar weld samples (Reproduced with permission).

Sample	Position 1	Position 2
Pristine		
Argon heat treated		
Air heat treated		

PCM heat treated		
Sample	Position 6	Position 7
Pristine		
Argon heat treated		
Air heat treated		



4.3.2 Crack analysis

Further analysis was complete into the PCM samples due to this scratching. When the dissimilar weld fractured, unpolished sample was analysed, surface level cracking could be seen as is shown in Figure 20. The SS 316L portions looked to have multiple small cracks and flaked away sections from the edges. Under the flaked sections a similar colouration to the pristine sample is observed, but it is lightly covered by a brown presumed to be corrosive layer. The Inconel 625 portion of the sample has multiple large cracks running through the entire surface. Further away from the weld darker sections appear to be present down the centre.

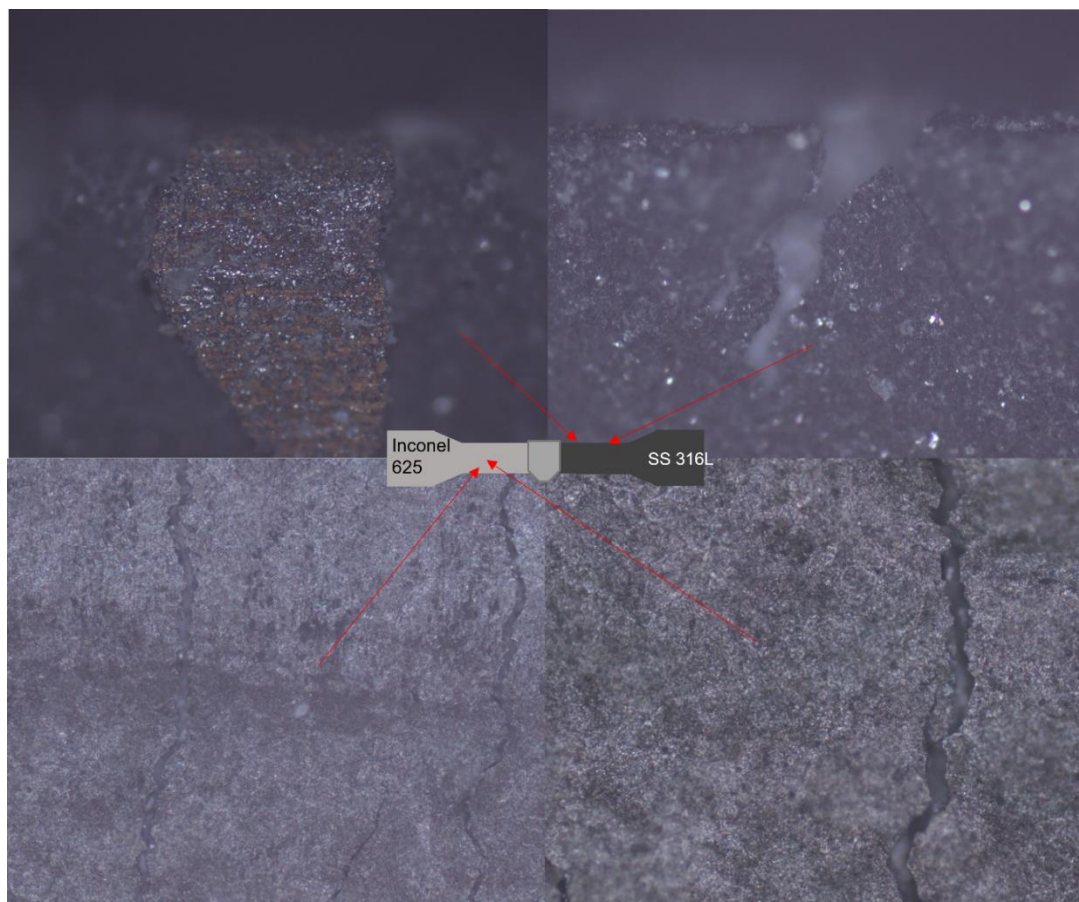


Figure 20 - PCM heat treated dissimilar weld sample without polishing. Cracking of stainless steel 316L (top) and Inconel 625 (bottom) sections.

4.3.3 Fracture analysis

The shape of each tensile fractured sample was also analysed, through both visual and optical microscopy methods. Examples of the dissimilar weld samples can be seen in Figure 21. The pristine sample fractured by necking considerably (backed up in section 4.2 by the greater ductility values) before fracture, where multiple dimples could be seen in the cross section. Argon, air and PCM heat treated samples fractured with little to no necking at a 45 degree angle. These fracture types were consistent with the SS 316L similar weld samples, but were not for Inconel 625 samples. The pristine sample did neck and form a dimpled fracture, but the argon and air heat treated samples had a linear fracture. When consulting literature [58, 59] dimples and necking represent a ductile fracture. This is expected for both SS 316L and Inconel 625 samples as they are relatively ductile materials. The 45 degree fracture indicates that the maximum shear stress was obtained. Due to the little necking and maximum shear stress, this sample indicates a brittle fracture. Other literature [60] agrees with this, stating that heat treatments make materials brittle, as was speculated in section 4.1. The linear/normal directional fracture indicates a position between ductile and brittle behaviour. An important note is that no fracture occurred at the welds. All fractures occurred in the bulk material, with the dissimilar sample occurring in the weaker SS 316L.



Figure 21 - Comparison of fracture positions for dissimilar weld samples. Pristine sample (left) argon heat treated (centre) and air heat treated (right).

4.3.4 Topography differences

The topography of each condition before polishing was applied, was analysed. Tables 21 and 22 show the dissimilar weld samples of pristine and PCM samples. When comparing similar positions roughness and scratches appear consistent. The greatest difference is present at

positions 6 and 7, where PCM samples have multiple levels. This indicates large sections have been added or removed from the sample during the treatment procedure.

4.4 SEM and EDX analysis

4.4.1 Element mapping

The main consideration for SEM and EDX analysis was the elemental mapping the weld lines around each sample. These were complete at both the 'butt weld' side and 'long weld' side. The most important points were considering the dissimilar weld samples from the bulk SS 316L to the Inconel 625 weldment. This will be covered first.

Figure 22 looks at the pristine sample. As the elemental mapping shows iron is located on the left whilst nickel and molybdenum is located on the right. This is expected as the SS 316L bulk material is located on the left and Inconel 625 weldment is on the right, and as Tables 1 and 2 showed SS 316L mainly consists of iron and Inconel 625 of nickel and molybdenum. Chromium is present over the entire sample, which again is expected as both materials should contain a high level. A small amount of carbon is present, but due to its position, is located on the epoxy resin. This is expected as very small amounts of carbon should be present, but these levels are too low to pick up on through EDX elemental mapping. Oxygen levels however are present over both the epoxy and weld.

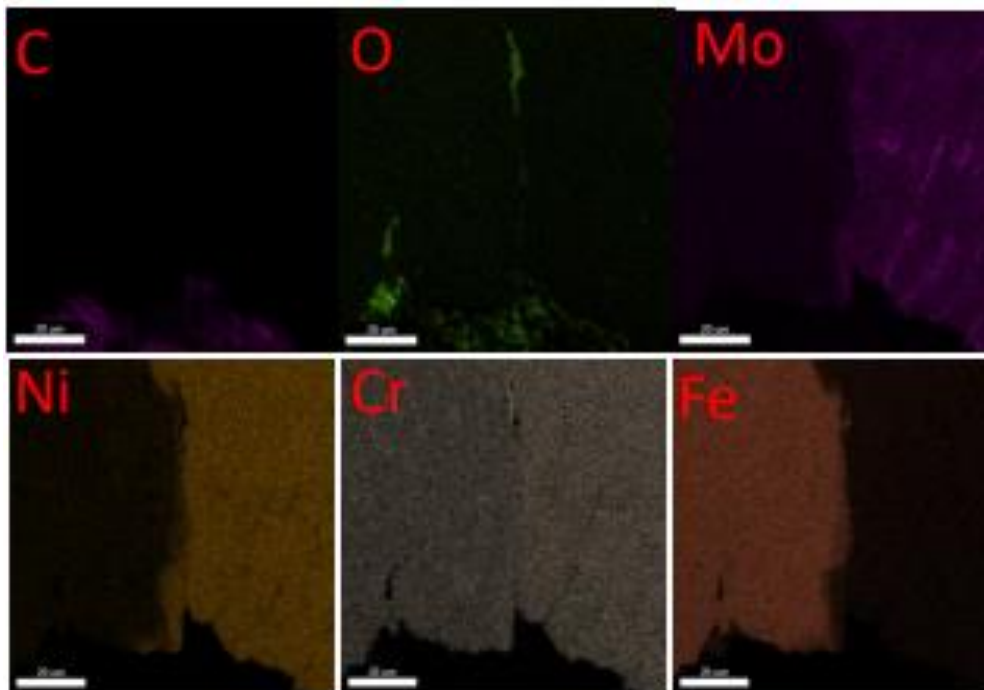
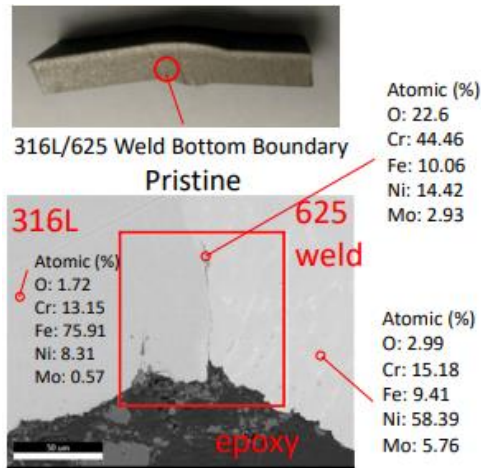


Figure 22 – Elemental mapping of the dissimilar weld’s pristine small samples cross section, located at the stainless steel 316L to weld line [55] (Reproduced with permission).

The argon heat treated sample, has the same elements present in the same positions. The only difference is the concentration of oxygen levels around the weld. All other concentrations of materials look to be relatively similar.

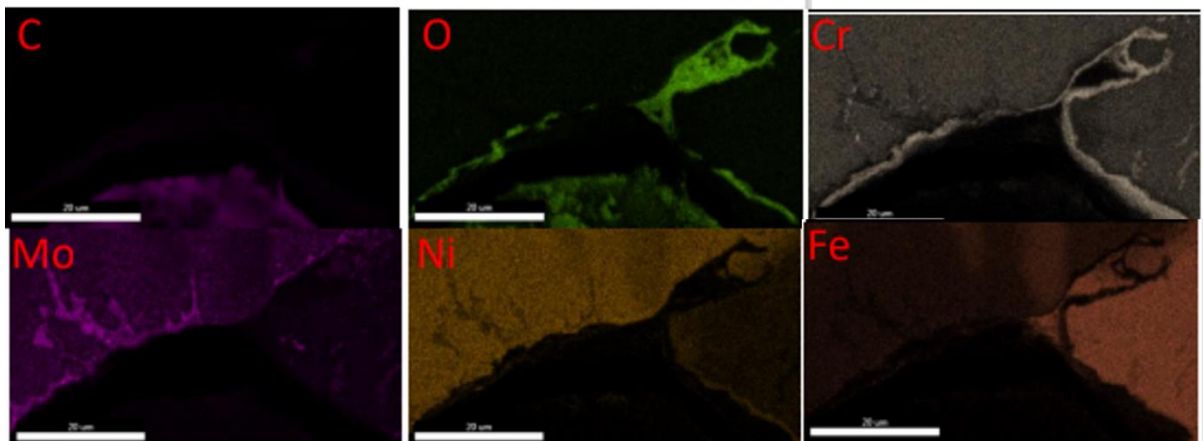
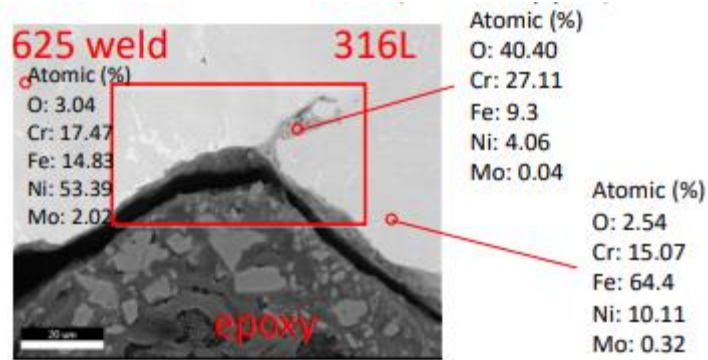


Figure 23 – Elemental mapping of the dissimilar weld’s argon heat treated small samples cross section, located at the stainless steel 316L to weld line [55] (Reproduced with permission).

Figure 24 considers the air heat treated sample. The reversed positions are seen for the iron and nickel. This is only due to the sample being in the reversed position (SS 316L on right, Inconel 625 on left). Chromium is consistent with previous, and carbon is flipped (sample orientation). Little molybdenum appears to be present, however when comparing the concentration values, a similar percentage is recorded. This is not the most accurate method of comparison however it does confirm the presence of the element. Most of the oxygen is present in the epoxy, however small layers look to be present over the entire sample. A greater concentration still resides around the weld. The red circle shows the top of the weld and how there is a greater oxygen concentration at this point, due to the more vibrant green colour.

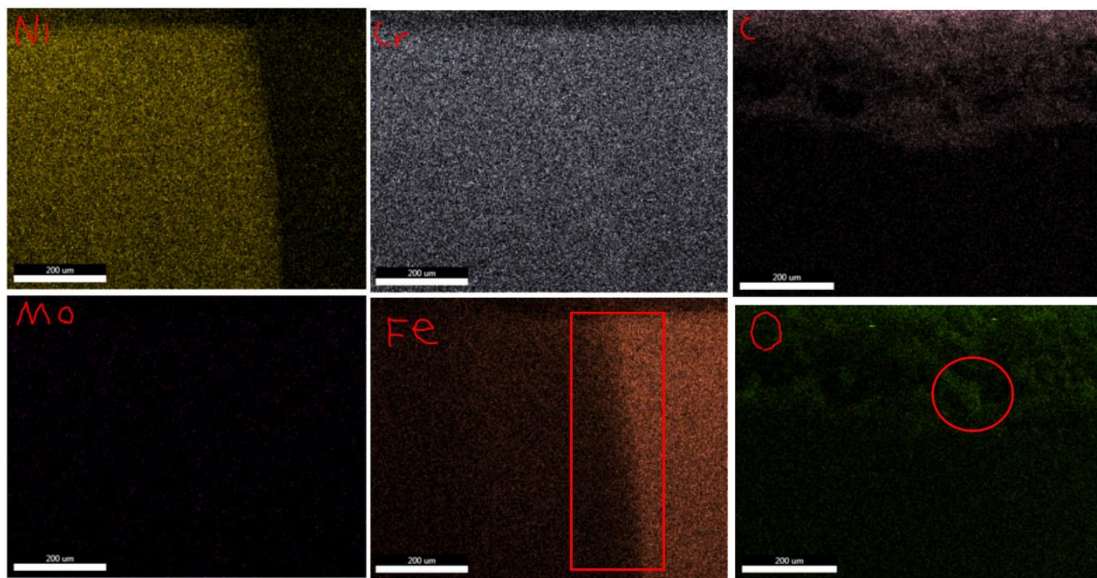
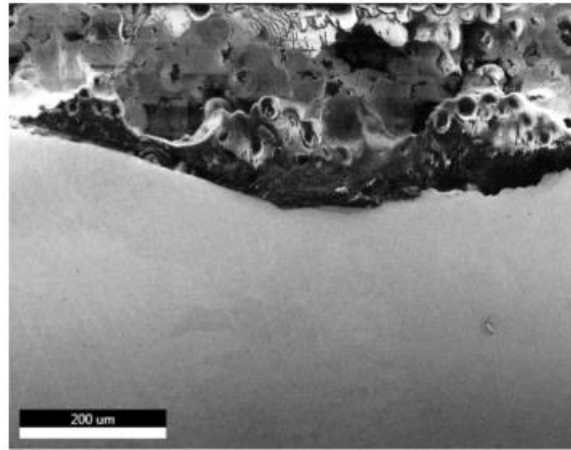


Figure 24 – Elemental mapping of the dissimilar weld’s air heat treated small samples cross section, located at the stainless steel 316L to weld line.

The PCM heat treated sample is considered last. This sample has the welded portion on the left, showing similar iron, nickel, molybdenum and chromium positions and concentrations to the air heat treated sample. The oxygen looks to be present over the entire sample, with greater concentrations around the weld line and Inconel 625 weldment. A similar pattern is followed by a sodium presence. This presence was not seen in any of the other samples. As according to Table 1 and 2 there should not be a notable sodium presence in the samples. The PCM heat treatment uses a sodium carbonate and potassium carbonate salts to conduct the test. As these samples are cut cross sections, the sodium is only present in this samples weld, it is possible that this treatment affects welds past the surface.

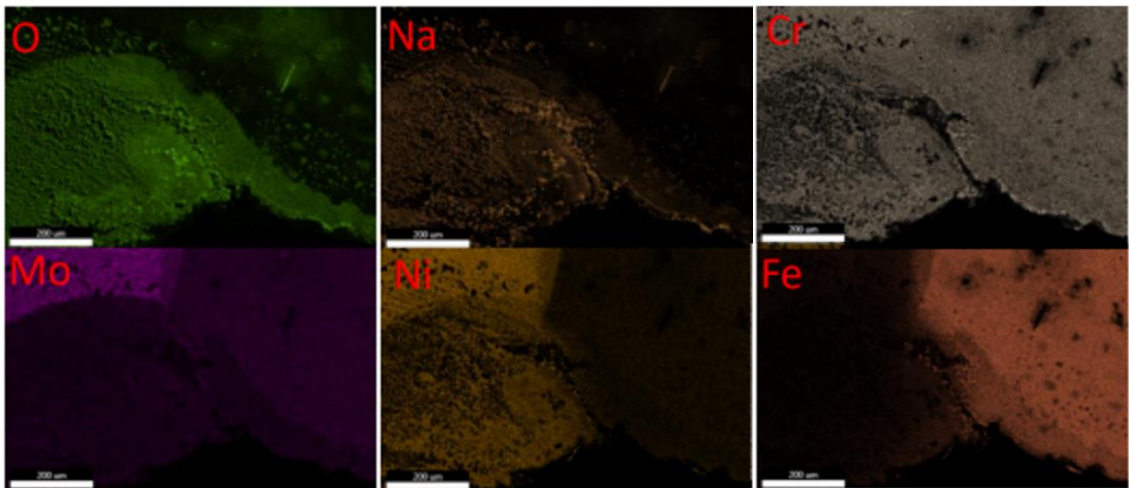
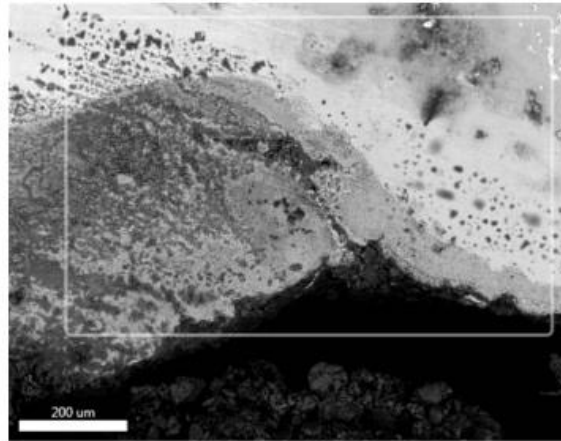


Figure 25 – Elemental mapping of the dissimilar weld’s PCM heat treated small samples cross section, located at the stainless steel 316L to weld line [55] (Reproduced with permission).

A couple of different trends were noticed. The weld line, in all samples has a greater oxygen content. Literature states this is a common occurrence [61]. The initial levels present in the sample increase the porosity of the weld, therefore increasing the chances of other impurities entering the weld during the welding process and any other subsequent heat treatments. Considering the PCM heat treated sample, this agrees with the idea that sodium could bring further oxidation throughout the entire weld.

The weld line also appears to consist of different concentrations to the weld and bulk material. The concentration levels appear to gradually decline from the maximums of one material to the minimums of the other material as is highlighted by the red box in Figure 24. This is most likely an instrumental inaccuracy due to the thickness of the weld reducing to a level where the bulk SS 316L material is being registered below the weld. Although unlikely, due to fracture from tensile stress tests not occurring at this position, if this is not

the reason and that the weld itself shares elemental concentrations near the weld line, mechanical properties would be negatively affected.

Three unpolished samples which can be seen in Figures 41, 42 and 43. These consider the surface cross section of air heat treated samples for all three configurations. For the dissimilar weld very similar concentrations of iron, nickel, molybdenum and chromium are present, with the same gradient at the weld line. Manganese was present at the Inconel 625 weld, which Table 2 confirms should occur. Small amounts of silicon and carbon are seen over the entire sample. These points are most likely small fragments left from the packaging due to their irregular consistencies and the unpolished surfaces topography. Differing from Figure 24 a high concentration of oxygen is also present over the entire sample. This indicates complete corrosion has occurred over the surface. This is expected due to it being an exterior surface which was exposed directly to the air heat treatment. For the SS 316L similar weld sample (Figure 43) similar concentrations of chromium and oxygen are present as is expected. Iron, nickel and molybdenum also are stated to be present. The nickel and molybdenum are much lower in concentration though, indicating only SS 316L is present as it should be. No large difference appears between the bulk material and weldment. The Inconel 625 similar weld also looks to have similar levels of oxidation, accompanied by sodium and carbon impurities/alien particles. The nickel, sulphur, chromium and iron concentrations are also consistent over the entire sample and agree with Table 2. Although unpolished these samples assist in showing that the welds and bulk material exterior are affected by treatments very similarly. This further highlights the abnormality of the oxygen and sodium presence only in the weldment of the PCM heat treatment sample, indicating a potential issue.

4.4.2 Thickness gain and thickness loss

The visible discolouration or colour differences from the exterior/edges of the sample, seen through SEM imaging, were measured to determine the material loss caused by the heat treatments. Positions 1 – 7 for dissimilar weld cross section samples were considered. Images taken and tabulated results can be found in the section 8.5, Tables 28 and 29. The results from this test are seen in Figure 26. The argon heat treatments produced little discolouration, air produces a good proportion more, but PCM heat treatments created the largest colour change by a good margin. These results are expected due to PCM creating the most hostile environment followed by air and then argon heat treatments. There was no consistent trend noted. Each sample looked to react differently. The HAZ of SS 316L was the greatest for

argon, bulk Inconel 625 for air and centre of weld for PCM. This lack of a trend is most likely down to the low accuracy method. As seen in Table 28 the colour change is not always obvious and does not always represent a vertical change. To obtain a more accurate representation methods such as weight loss could be applied.

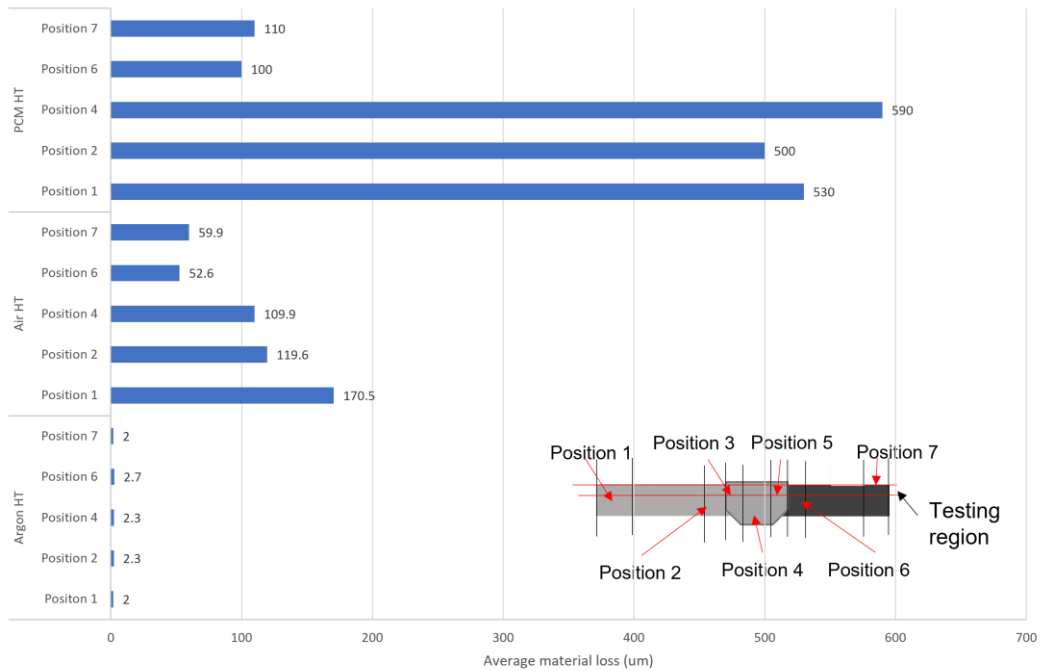


Figure 26 – Chart comparing the material loss at positions 1, 2, 4, 6 and 7 for all heat treatments of dissimilar weld small samples.

Material gain was also calculated through the level of corrosion present in each sample. This was measured at each weld line through the oxygen encroachment distance. These results that can be seen in Figure 27, follow a similar pattern to the material loss chart (Figure 26).

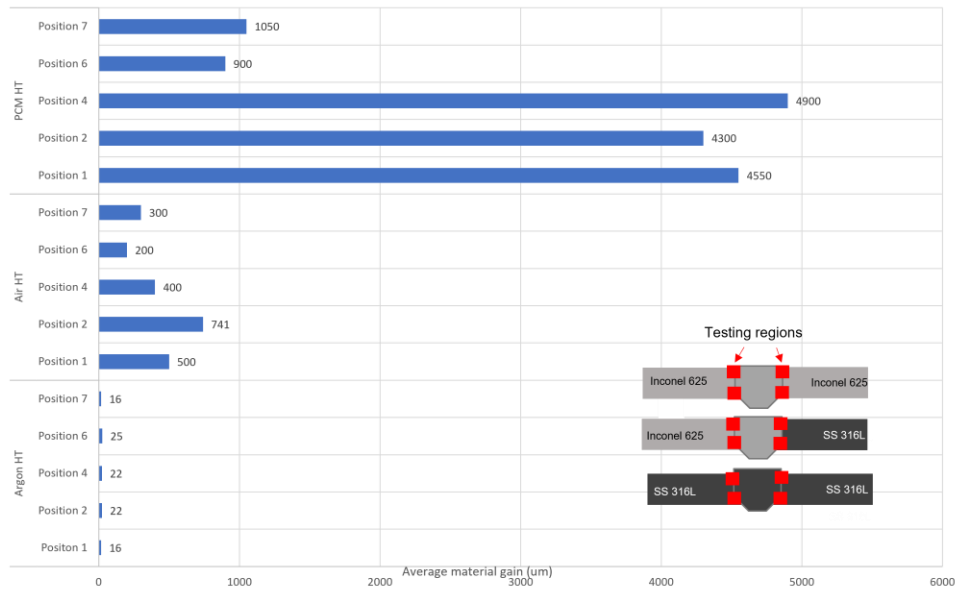


Figure 27 - Chart comparing the material gain at positions 1, 2, 4, 6 and 7 for all heat treatments of dissimilar weld small sample.

5. Discussion

The discussion will consider some of the unanswered or more detailed points of the results. Limitations and issues with the overall testing procedure or results will also be considered here.

5.1 Bent samples

After the welded plates were received, it was noted that all the plates were bent, with the greatest being around 11 degrees. An example of this can be seen in Figure 28. Once the dogbones and small samples were cut this bend was attempted to be removed through heat being applied to the weld whilst the sample was slowly straightened. This was only complete for the dogbones, with small samples being left as they were received. As an extra thermal aspect has been introduced, there is a possibility that the results are not completely accurate. Literature on the effects of multiple heat treatments [62] shows that after many heat treatments, the positive affects become negative mating the material typically weak a brittle.

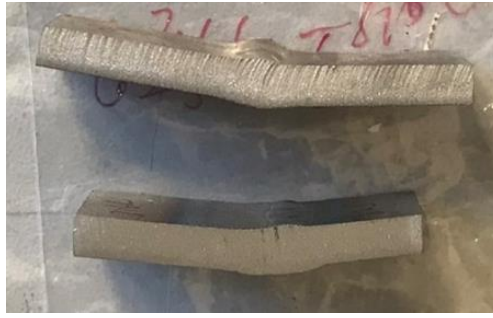


Figure 28 – Example of bent sample.

5.2 Fracture position - tensile

As was stated in section 4.3.3 it was noted in all tests that the fracture of all dogbones in the tensile stress test did not occur at the weld. As illustrated in Table 8 found in section 8.2 of the appendix, and Figure 29 all fractures occurred at approximate the centre (with around a 15% discrepancy) of the bulk material. In the dissimilar weld samples this failure occurred in the SS 316L portions of the samples. The similar weld samples predominantly failed at the top side (side at the higher elevation in the Instron tensile testing equipment). The most similar literature also showed these effects [43, 44, 45]. Through research the understanding was that the welded section could only be as strong as the bulk material, but no stronger [63]. It is theorised that the welds are in fact the opposite and act as a point of increased tensional strength. As was stated in the literature review with the tensile stress results agreeing, heat treatments increase the tensile strength and stiffness whilst reducing the ductility. As the process of welding applies a localised high temperature, it is possible that a small change in the metal's alignment occurred, removing gaps or impurities from the structure. It is also possible that the forward push method of applying the weldment, is better aligned than the bulk material, thus reducing its deformities and increasing the strength.



Figure 29 – Pristine and argon heat treated dogbone samples, before (left) and after (right) the tensile strength test.

5.3 Colour changes after PCM heat treatment

At the end of the PCM testing it was noted that some of the PCM salt was still present in the crucibles, as seen in Figure 30. When removing the samples some notable differences in colour were seen with darker sections having been the buried sections. This is due to the PCM being stagnant and thus differently packed sections will potentially liquify quicker. The samples possessed a worse tensile strength and ductility accompanied by increased stiffness and hardness compared to both the pristine and other treated samples. These different properties are expected as literature states [64] that these decreases should occur however the levels are not referred to. Therefore, it is possible that this colour difference represents uneven levels of exposure, which could have altered the stress and levels of corrosion. In CSTP systems the PCM has a driven flow rate which does not allow for stagnation and this accumulating affect to occur as commonly. Emergency procedures for when these flow rates are affected/broken could want to understand this effect further.



Figure 30 – Presence of solid PCM remaining after heat treatment.



Figure 31 – PCM heat treated dogbone samples. Dissimilar weld front (left) and back (centre), accompanied with front image of stainless steel 316L similar sample (right).

5.4 PCM flaking

In sections 4.1 and 4.3 differences in external layers of both materials in PCM samples was observed. Inconel 625 sections appeared to have outside layer whilst SS 316L looked to flake instead. Literature suggests these are oxide layers, with the Inconel 625 creating a chromium oxide [65] whilst SS 316L creates a chromium oxide and iron oxide [66]. The weldments also appear to create the same plates and flaking at very similar rates. The Inconel 625 plates have a considerably greater thickness than the SS 316L flaking. When no loads are applied the oxidised plates remains consistent whilst the thinner flaking layer would still slowly break away. This demonstrates why Inconel 625 has better chemical resistances, as literature previously stated. This protective layer however, broke at a considerably lower tensile strength (around 200 MPa) and was recorded to have much lower hardness levels, as can be seen in Table 16 and 17. No literature could be found to compare these values. This weakness therefore highlights the importance of reducing the potential for unconsidered forces to affect this dissimilar weld, when in corrosive environments.



Figure 32 – PCM heat treated dissimilar weld sample after fracture. Inconel 625 to weld cross section (left). Coving plate broken away from Inconel 625 (centre). Flaking of stainless steel 316L (right).

5.5 Limitations

Throughout the research and testing phase, multiple limitations have been discovered. Some were overcome with no issue, others produced a result, but its accuracy is questionable whilst others could not be resolved. Two of the main unresolved issues are the level of repetitions and non-polished samples which underwent hardness testing and characterisation.

The fractured samples (dogbone samples after undergoing tensile stress tests) all underwent Vickers hardness tests. These samples were anywhere from 70 mm to 130 mm in length, making them considerably larger than samples which can fit in the Struers's polishing machine. Each sample could have been cut down into three separate sections (position 1 and 7 on their own, with positions 2 to 6 in one sample) and polished. This would have required for six cuts to be made in every sample, equating to 80 cuts overall. Two or three of these cuts can be made per day, giving a 27-40 day waiting time for the samples to be prepared at a minimum. Due to the IsoMet saw being required for other projects this would have taken longer, making it impossible to complete. The results obtained by these unpolished surfaces were therefore not as accurate for the hardness testing, SEM and EDX imaging. Exact values and complete analysis could therefore not be complete for these tests.

In this report one set of samples for each test was sourced and prepared. This only allowed for observations of a single test to be made. Limited comparison and no extensive level of error to calculate the accuracy and precision could be made. The time and available resources made it impossible to obtain and test further samples. With this further testing the points

brought forth in this report could be further speculated, helping to either confirmed or deny the trends.

6. Conclusions

This study aimed to increase the available knowledge on dissimilar welds between stainless steel 316L and Inconel 625. As has been covered, the researched literature showed that both materials properties and the possibilities of dissimilar welding has been previously researched, but not all aspects have been simultaneously considered. This left a large literature gap which this study has covered. The proposed methodology utilised previous literatures methods, allowing for result to be compared. The different testing conditions where developed to create both a baseline of temperature and chemical influences and a worst case simulation for the dissimilar weld, whilst being used in the CSTP. Tests and there results based around the tensile strength, Young's modulus, ductility, Vickers hardness, grain sizes, oxidation levels, elemental concentrations and elemental locations, were gathered through the previously stated methods. The main outcomes from these points are;

- 1) Fracture never occurs at the weld.
- 2) Tensile strength and ductility are not affected by the presence of a dissimilar weld.
The 'worse' bulk materials tensile strength and ductility represent the overall dissimilar weld sample.
- 3) The presence of a weld reduces the stiffness by a significant amount. This level considerably increases with dissimilar welds.
- 4) Surface level oxidation is consistent over bulk materials and dissimilar welds
- 5) Highly corrosive treatments are potentially intrusive through the Inconel 625 weldment and affect all mechanical properties poorly.

Some of the results and further observations which were made, where covered in the discussion. The initial condition of the samples, colour change after each treatment and causes of flaking after PCM treatments were speculated upon as literature did not provide any relevant comparisons.

Overall the study has provided further understanding into the properties of dissimilar welds between SS 316L and Inconel 625. Furthermore, a series of questions have also been discovered and that potential future work can be seen below.

6.1 Future work

For the understanding of dissimilar welds, there is more researched and testing which can be complete to give a more defined understanding of relevant chemical and mechanical behaviours.

6.1.1 Completion of tests

At the beginning of this report the solar thermal system, was described being constructed from large tanks and pipes. The dogbone and small samples are linear in geometry and therefore make a good simulation of the tanks structure, but not the pipes. The same tests and characterisation process being complete on tubular samples would give a further understanding to the dissimilar weld's properties. It would assist in understanding weather geometry creates a difference to the weld's strength, ductility, and hardness.

In the methodology every test and characterisation were stated to be complete on all samples at each position. Ultimately for this report, this did not occur due to time restraints and equipment usage for other projects. Some Vickers hardness tests were half complete for similar weld samples due to the time constraints. This is due to positions 1 – 3 should be the same as 5 – 7 for similar weld samples. To produce more accurate and detailed results, all position s should still have been tested. The same situation occurred with EDX elemental mapping. Little remaining time and availability of the equipment, required for tests to be cut short.

6.1.2 Different conditions

In this report a single thermal condition of 750 degrees centigrade was considered, as it is deemed a median ground of temperatures present in CSTP systems. This was done to allow for accurate comparisons to be made between each sample. CSTP systems however can get considerably hotter than this and can remain so for longer than 500 hours. The repetition of these tests and characterisation should therefore be conducted at different temperatures and durations to find any differences. With this information rates of change and difference will be capable of being calculated, allowing for yearly material loss to be determined for the system.

Similarly, more accurate conditions could be implemented such as the exact sodium phase change material that CSTP systems utilise. Simultaneously small-scale tests with the correct geometry of the CSTP system could also be tested to determine if different levels of stress are applied to the dissimilar welds in the desired configuration. The effects of flow rate, thermal fluidity and continuous production could also be observed and tested.

6.1.3 Different mechanical tests

As a direct continuation from this report, other mechanical properties could be tested. The three next most important and relevant are creep, bending and fatigue. Creep measures the level of strain which a material experiences whilst a constant temperature and load is being applied. Bending tests have a constant force applied and the flexural strength is measured. Both the creep and bending properties relate to CSTP as the pipes and tanks which are heated, are located underground, and will experience a constant force/pressure. Fatigue tests repeatedly apply and remove a load until fracture, allowing for lifetime measurements to be obtained. Surrounding areas of CSTP systems could be moving therefore changing the experienced pressure. Fatigue tests assist in determining the effects this could have.

6.1.4 Different imaging

As seen in this report optical microscopy, SEM and EDX imaging techniques have been utilised. These techniques are defined as surface level observation and characterisations methods. These methods can therefore only see what the exterior of the sample is experiencing. Micro CT is a non-intrusive characterisation technique which takes internal segmented images of samples. This would allow for samples internal structures to be observed. This information could differ to that obtained by taking a cross section cut, thus giving a greater understanding of the weld's configuration. An example of where this may be useful is determining if under the top layer after PCM heat treatment does alter the mechanical properties.

7. References

1. W.H. Meng, 2022. “Solar energy”. National Geographic, Available at; <https://education.nationalgeographic.org/resource/solar-energy>. [Accessed 14/3/2022]
2. S. Hurley, 2019. “Solar energy”. Explaining science. Available at; <https://explainingscience.org/2019/03/09/solar-energy/>. [Accessed 14/3/2022]
3. N. Fletcher, 2015. “The energy we get free from the sun is free and abundant. How do we harness it?”. Australian Academy of Science, Available at; <https://www.science.org.au/curious/technology-future/solar-pv>. [Accessed 14/3/2022]
4. Boerema, N., Morrison, G., Taylor, R. and Rosengarten, G., 2012. “Liquid sodium versus Hitec as a heat transfer fluid in solar thermal central receiver system”. Solar Energy, 86, pp. 2293-2305. [Accessed 14/3/2022]
5. B. Belgasim, M. Elmnefi, 2014. “Evaluation of a Solar Parabolic Trough Power Plant under Climate Conditions in Libya”. Mechanical Engineering department of Benghazi. Available at; https://www.researchgate.net/figure/Schematic-of-a-concentrated-solar-thermal-parabolic-trough-power-plant-with-thermal_fig1_269095678. [Accessed 17/3/2022]
6. C. Riesgo, 2022. “AISI type 316L stainless steel, annealed bar”. ASM aerospace specification metals incorporated, Available at; <https://asm.matweb.com/search/SpecificMaterial.asp?bassnum=mq316q>. [Accessed 17/3/2022]
7. Oliveira, M.M.D., Couto, A.A., Almeida, G.F.C, Reis, D., Lima, N.D. and Baldan, R., 2019. “Mechanical behaviour of Inconel 625 at elevated temperatures”. Metals – open access metallurgy journal, 9, pp. 3-301. [Accessed 27/3/2022]
8. N. Douse, 2022. “Inconel 625”. Waverly Brownall, Available at; <https://waverleybrownall.co.uk/inconel-625/>. [Accessed 4/4/2022]
9. A. Velling, 2019. “Mechanical properties of materials”. Fractory, Available at; [https://fractory.com/mechanical-properties-of-materials/#:~:text=From%20those%20two%20concepts%20we,suitability%20for%20a%20certain%20application\).&text=Stiffness%20is%20expressed%20as%20Young's,known%20as%20modulus%20of%20elasticity](https://fractory.com/mechanical-properties-of-materials/#:~:text=From%20those%20two%20concepts%20we,suitability%20for%20a%20certain%20application).&text=Stiffness%20is%20expressed%20as%20Young's,known%20as%20modulus%20of%20elasticity). [Accessed 4/4/2022]

10. MechaniCalc, 2022. “*Mechanical properties of materials*”. MechaniCalc, Available at; <https://mechanicalcalc.com/reference/mechanical-properties-of-materials>. [Accessed 4/4/2022]
11. Sharpe, W.N., 2001. “*Mechanical properties of MEMS materials*”. The MEMS handbook, 3, pp. 1-33. [Accessed 4/4/2022]
12. J.O.d Beeck, 2022. “*Description of mechanical properties*”. Arcelor Mittal, Available at; https://industry.arcelormittal.com/repository/fce/PDF-technical-chapters/Prcat_Descriptionofmechanicalproperties.pdf. [Accessed 16/4/2022]
13. University of Washington, 2022. “*5. Mechanical properties and performance of materials*”. University of Washington, Available at; <https://courses.washington.edu/me354a/chap5.pdf>. [Accessed 16/4/2022]
14. A. Ghosh, 2004. “*Stainless steel – Grade 316L – properties, fabrication and applications*”. AZO Materials, Available at; <https://www.azom.com/article.aspx?ArticleID=2382>. [Accessed 20/6/2022]
15. D.O. Kipp, 2022. “*Stainless steel 316L*”. MatWeb, Available at; <https://www.matweb.com/search/DataSheet.aspx?MatGUID=9e9ab696974044cab4a7fd83687934eb&ckck=1>. [Accessed 18/4/2022]
16. R. Yano, 2022. “*AISI 316L stainless steel properties, composition, tensile yield strength*”. Material world, Available at; <https://www.theworldmaterial.com/aisi-316l-stainless-steel/>. [Accessed 28/6/2022]
17. D. Popescu, 2022. “*316 stainless steel mechanical properties*”. EZ lok, Available at; <https://www.ezlok.com/316-stainless-steel-properties>. [Accessed 28/6/2022]
18. A. Ghosh, 2012. “*Super alloy altemp625 (UNS No6625)*”. AZO materials, Available at; <https://www.azom.com/article.aspx?ArticleID=7796>. [Accessed 28/6/2022]
19. D.O. Kipp, 2022. “*MetalTek MTWK 625 cast UNS N26625 service corrosion and heat resistance alloy*”. MatWeb, Available at; <https://www.matweb.com/search/DataSheet.aspx?MatGUID=748762b96b494162b4b6a2f2c0a1b1f1>. [Accessed 28/6/2022]
20. C. Riesgo, 2022. “*Special metals Inconel alloy 625*”. ASM aerospace specification metals Inc, Available at; <https://asm.matweb.com/search/SpecificMaterial.asp?bassnum=NINC33>. [Accessed 28/6/2022]

21. M. Donegan, 2022. “*Inconel alloy 625*”. Special metals, Available at; <https://www.specialmetals.com/documents/technical-bulletins/inconel/inconel-alloy-625.pdf>. [Accessed 28/6/2022]
22. Roberts, D.I., Ryder, R.H. and Viswanathan, R., 1985, “*Performance of dissimilar welds in service*”. Journal of Pressure Vessel Technology, 3, pp. 247-254. [Accessed 2/5/2022]
23. Joseph, A., Rai, S.K, Jayakumar, T. and Murugan, N., 2005. “*Evaluation of residual stresses in dissimilar weld joints*”. International journal of pressure vessels and piping, 82, pp. 700-705. [Accessed 2/5/2022]
24. R.E. Avery, 1991. “*Guidelines for welding dissimilar metals*”. Nickel development institute, Available at; https://nickelinstitute.org/media/1691/guidelinesforweldingdissimilarmetals_14018_.pdf. [Accessed 21/5/2022]
25. ASSDA, 2002. “*Welding dissimilar metals*”. Australian stainless steel development association, Available at; <https://www.assda.asn.au/images/PDFs/FAQs/FAQ9.pdf>. [Accessed 21/5/2022]
26. Kumar, N., Yuan, W. and Mishra, W.S, 2015. “*Chapter 2 – A framework for friction stir welding of dissimilar alloys and materials*”. Friction Stir Welding of Dissimilar Alloys and Materials, 1, pp. 15-33. [Accessed 27/5/2022]
27. CSIRO, 2022. “*Concentrated solar thermal research*”. Australia’s national science agency, Available at; <https://www.csiro.au/en/research/technology-space/energy/solar-thermal>. [Accessed 27/5/2022]
28. K. Lovegrove, G. Nathan, J. Zapata, 2016. “*Concentrating solar thermal*”. Australian Academy of Science, Available at; <https://www.science.org.au/curious/technology-future/concentrating-solar-thermal#:~:text=The%20concentrated%20radiation%20absorbed%20by,cause%20the%20receiver%20to%20melt.>. [Accessed 2/6/2022]
29. Mei, D., Lamaka, S.V., Lu, X. and Zheludkevich, M.L., 2020. “*Selecting medium for corrosion testing of bioabsorbable magnesium and other metals – A critical review*”. Corrosion Science, 171, pp. 1-14. [Accessed 2/6/2022]
30. Laque, F.L., 1956. “*Theoretical studies and laboratory techniques in sea water corrosion testing evaluation*”. Corrosion - the journal of science & engineering, 13, pp. 33-44. [Accessed 2/6/2022]

31. Moteshakker, A. and Danaee, I., 2016. “*Microstructure and corrosion resistance of dissimilar weld joints between duplex stainless steel 2205 and austenitic stainless steel 316L*”. *Journal of Materials Science & Technology*, 22, pp. 282-290. [Accessed 10/9/2022]
32. Liqing, H., Guobiao, L., Zidong, W., Hong, Z., Feng, L. and Long, Y., 2010. “*Study on corrosion resistance of 316L stainless steel welded joint*”. *Rare Metal Materials and Engineering*, 39, pp. 393-396. [Accessed 10/9/2022]
33. Dadfar, M., Fathi, M.H., Karimzadeh, F., Dadfar, M.R. and Saatchi, A., 2006. “*Effect of TIG welding on corrosion behaviour of 316L stainless steel*”. *Materials Letters*, 61, pp. 2343-2346. [Accessed 18/6/2022]
34. Ma, C., Peng, Q., Mei, J., Han, E.H. and Ke, W., 2018. “*Microstructure and corrosion behavior of the heat affected zone of a stainless steel 308L-316L weld joint*”. *Journal of material science & technology*, 34, pp. 1823-1834. [Accessed 18/6/2022]
35. Kumar, S.S., Murugan, N. and Ramachandran, K.K., 2017. “*Microstructure and mechanical properties of friction stir welded AISI 316L austenitic stainless steel joints*”. *Journal of Materials Processing Technology*, 254, pp. 79-90. [Accessed 18/6/2022]
36. Sabzi, M., Mousavi, S.H., Eivani, A.R., Park, N. and Jafarian, H.R., 2021. “*The effect of pulse current changes in PCGTAW on microstructural evolution, drastic improvements in mechanical properties, and fracture mode of dissimilar welded joint of AISI 316L AISI 310S stainless steels*”, *Materials science and engineering*, 823, pp. 2-8. [Accessed 30/7/2022]
37. Khidhir, G.I. and Baban, S.A., 2019. “*Efficiency of dissimilar friction welded 1045 medium carbon steel and 316L austenitic stainless steel joints*”. *Journal of materials research technology*, 8, pp. 1926-1932. [Accessed 30/7/2022]
38. Vemanaboina, H., Gundabattini, E., Akella, S., Rao, A.C.U.M., Buddu, R.K., Ferro, P. and Berto, F., 2021. “*Mechanical and metallurgical properties of CO2 laser beam Inconel 625 welded joints*”. *MDPI*, 1, pp. 2-6. [Accessed 19/7/2022]
39. Sivakumar, J., Korra, N.N. and Vasantharaja, P., 2020. “*Computation of residual stresses, distortion, and thermogravimetric analysis of Inconel 625 weld joints*”. *Sage journals*, 235, pp. 110-116. [Accessed 3/8/2022]

40. Corigliano, P. and Crupi, V., 2021. “*Fatigue analysis of Ti6Al4V/Inconel 625 dissimilar welded joints*”. Ocean engineering, 221, pp. 3-5. [Accessed 3/8/2022]
41. Oliveira, M.M.D., Couto, A.A., Almeida, G.F.C. and Reis, D., 2019. “*Mechanical behaviour of Inconel 625 at elevated temperatures*”. Metals – Open Access Metallurgy Journal, 9, pp. 301. [Accessed 3/8/2022]
42. Gou, L., Zheng, H., Liu, S., Li, Y., Feng, C. and Xu, X., 2016. “*Effect of heat treatment temperatures on microstructure and corrosion properties of Inconel 625 weld overlay deposited by PTIG*”. International journal of electrochemical science, 11, pp. 5507-5519. [Accessed 10/8/2022]
43. Kulkarni, A., Dwivedi, D.K. and Vasuevan, M., 2020. “*Microstructure and mechanical properties of A-TIG welded AISI 316L SS-alloy 800 dissimilar metal joints*”. Materials science and engineering, 790, pp. 3-6. [Accessed 10/3/2022]
44. Kumar, K.G., Devendranath, K. and Arivazhagan, N., 2015. “*Characterization of metallurgical and mechanical properties on the multi-pass welding of Inconel 625 and AISI 316L*”. Journal of mechanical science and technology, 29, pp. 1039-1047. [Accessed 10/8/2022]
45. Ramkumar, T., Selvakumar, M., Narayanasamy, P., Begam, A.A., Mathavan, P. and Raj, A.A., 2017. “*Studies on the structural property, mechanical relationships and corrosion behaviour of Inconel 718 and SS 316L dissimilar joints by TIG welding without using activated flux*”. Journal of manufacturing processes, 30, pp. 290-298. [Accessed 25/8/2022]
46. G. Fry, 2022. “*Pan-industry welding management service*”. Technoweld, Available at; <https://technoweld.com.au/services/>. [Accessed 25/8/2022]
47. Standards Australia, 2020. “*Pressure equipment – welding and brazing qualifications*”. Intertek SAI global standards, Available at; https://infostore.saiglobal.com/en-us/standards/as-3992-2020-122295_saig_as_as_2845463/. [Accessed 25/8/2022]
48. Yin, Y., Andersson, G., Griesser, A. and Hashemi, R., “*The behaviour of Inconel 625 and stainless steel 316L weldment at elevated temperature in Phase Change Material (PCM) or for Concentrated Solar Plant Applications*”. Unpublished. [Accessed 10/4/2022]
49. S. Scheiber, 2022. “*IsoMet low speed saw*”. Buehler, Available at; <https://www.buehler.com/assets/Brochures/English/Sectioning/IsoMetLowSpeedSaw.pdf>. [Accessed 25/8/2022]

50. Butt, J., Hewavidana, Y. and Mohaghegh, S.S.E., 2019. “*Hybrid manufacturing and experimental testing of glass fiber enhanced thermoplastic composites*”. *Journal of manufacturing and materials processing*, 3, pp. 96. [Accessed 6/9/2022]
51. N. Hunn, 2022. “*Metallographic preparation of stainless steel*”. Struers, Available at; <https://www.struers.com/en/Knowledge/Materials/Stainless-Steel#grinding>. [Accessed 6/9/2022]
52. E.A. Maier, 2022. “*Minimum distance between test points and to the specimen edge*”. EMCO test, Available at; <https://www.emcotest.com/en/the-world-of-hardness-testing/hardness-know-how/applications-tips/general-tips/minimum-distance-between-test-points-and-to-the-specimen-edge/>. [Accessed 6/9/2022]
53. A. Sinfield, 2022. “*Product data sheet Nickel alloys*”. Austral Wright metals, Available at; [Inconel Alloy 625 | Austral Wright](#). [Accessed 6/9/2022]
54. Hou, Y., Lei, D., Yang, W. and Li, C., 2016. “*Experimental investigation on corrosion effect on mechanical properties of buried metal pipes*”. *International journal of corrosion*, 2016, pp. 3-7. [Accessed 6/9/2022]
55. Yin Y., “*Analysis of 316L-625 Welds Isothermally Exposed to Ar and PCM Environment*”. Unpublished, Available at; file:///C:/Users/Daniel/Downloads/316L%20625%20welds%20analysis-Key%20information%20collection%20V7%20(1).pdf . [Accessed 10/4/2022]
56. Nielsen, C.V. and Martins, P.A.F., 2021. “*Grain boundary area*”. *Metal Forming*, 2, pp. 7-107. [Accessed 28/9/2022]
57. Baltzer, N. and Copponnex, T., 2014. “*Grain size*”. *Precious Metals for Biomedical Applications*, 1, pp. 3-36. [Accessed 6/9/2022]
58. Pineau, A., Benzerga, A.A. and Pardoën, T., 2016. “*Failure of metals I: Brittle and ductile fracture*”. *Acta Materialia*, 107, pp. 424-483. [Accessed 30/9/2022]
59. Sundaram K.M., 1982, “*Fracture orientation*”. *Development in petroleum science*, 75, pp. 37-55. [Accessed 25/8/2022]
60. Stewart, M., 2021. “*Brittle fracture*”. *Surface production operations*, 5, pp. 93-116. [Accessed 25/8/2022]
61. Zou, Y., Ueji, R. and Fujii, H., 2013. “*Effect of oxygen on weld shape and crystallographic orientation of duplex stainless steel weld using advanced A-TIG (AA-TIG) welding method*”. *Materials characterization*, 91, pp. 42-49. [Accessed 28/9/2022]

62. Bott, I.D.S. and Teixeira, J.C.G., 1999. “*Toughness evaluation of a shield metal arc carbon manganese steel welded joint subjected to multiple post weld heat treatment*”. *Journal of materials engineering and performance*, 8, pp. 683-692. [Accessed 2/10/2022]
63. Shi, Y.J., Wang, L., Wang, Y.Q., Ma, J.S. and Bai, R.S., 2011. “*Finite element analysis of the combined connection with bolts and welds*”. *Applied Mechanics and Materials*, 94, pp. 316-321. [Accessed 2/10/2022]
64. Chang, L.C. and Read, T.A., 2017. “*Plastic deformation and diffusionless phase changes in metals – the Gold-Cadmium beta phase*”. *The Journal of The Minerals, Metals & Materials Society*, 3, pp. 47-52. [Accessed 2/10/2022]
65. Malafaia, A.M.D.S., Oliveira, P.B.D., Romain, L.L., Wouters, Y. and Baldan, R., 2020. “*Isothermal oxidation of Inconel 625 superalloy at 800 and 1000^oC: microstructure and oxide layer characterisation*”. *Materials Characterization*, 161, pp. 3-6. [Accessed 10/10/2022]
66. Huang, X., 2020. “*Oxidation behaviour of 316L austenitic stainless steel in high temperature air with long term exposure*”. *Materials Research Express*, 7, pp. 2-10. [Accessed 10/10/2022]

8. Appendices

8.1 Manuscript

The research and results generated and used in this report are to be used to create a manuscript. This manuscript is currently in the early stages of drafting with the results from the stress testing and hardness testing of polished samples, accompanied by the grain boundary and elemental mapping analysis, being used. Only factual evidence will be portrayed in this manuscript, with most points made in the discussion of this study remaining speculation for the specific question of “*Investigating mechanical properties of dissimilar welds of stainless steel 316L and Inconel 625 for high temperature corrosion application*”.

8.2 Tensile stress

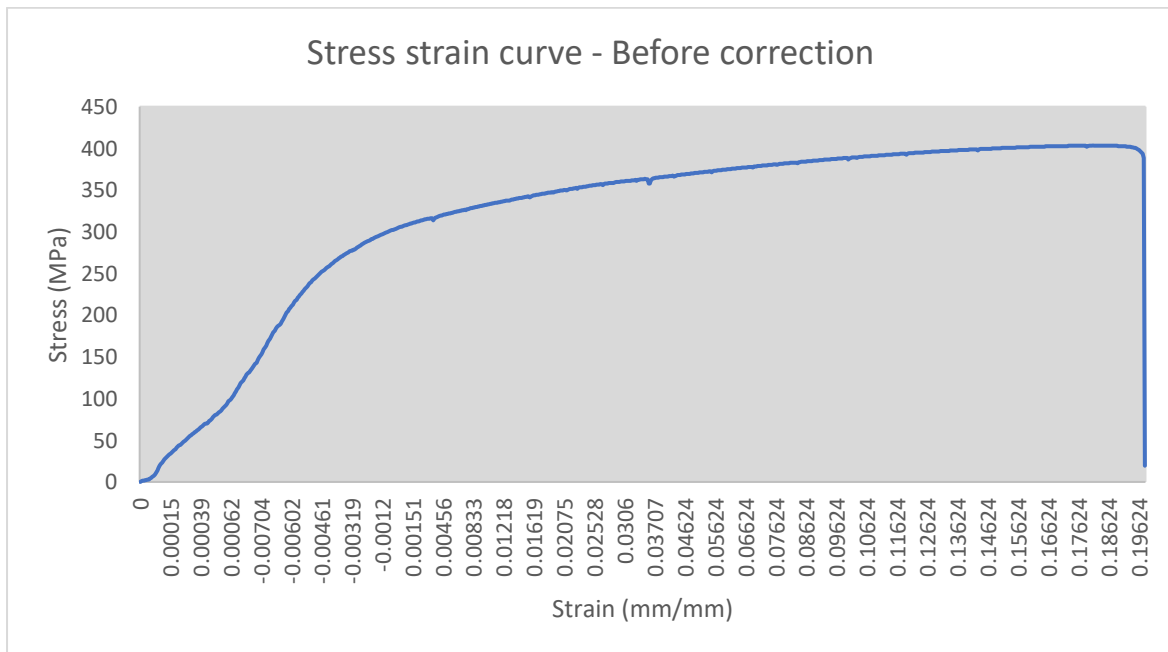


Figure 33 – Stress strain curve of PCM heat treated dissimilar weld sample, before correction was applied.

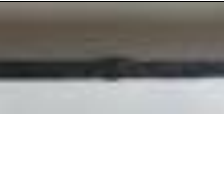
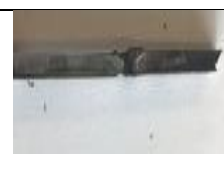
$$e_f = (L_f - L_0)/L_0$$

Calculation 1 – Elongation/ductility

$$E = \frac{\sigma}{\epsilon} = (y_2 - y_1)/(x_2 - x_1)$$

Calculation 2 – Youngs modulus

Table 8 - Dissimilar weld dogbone samples before and after fracture.

	Top face	Left (rotate to above top face)	Bottom face	Right (rotate to below top face)
Pristine before fracture				
Pristine after fracture				
Argon heated before fracture				
Argon heated after fracture				
Atmosphere heated before fracture				
Atmosphere heated after fracture				
PCM treated before fracture				
PCM treated after fracture				

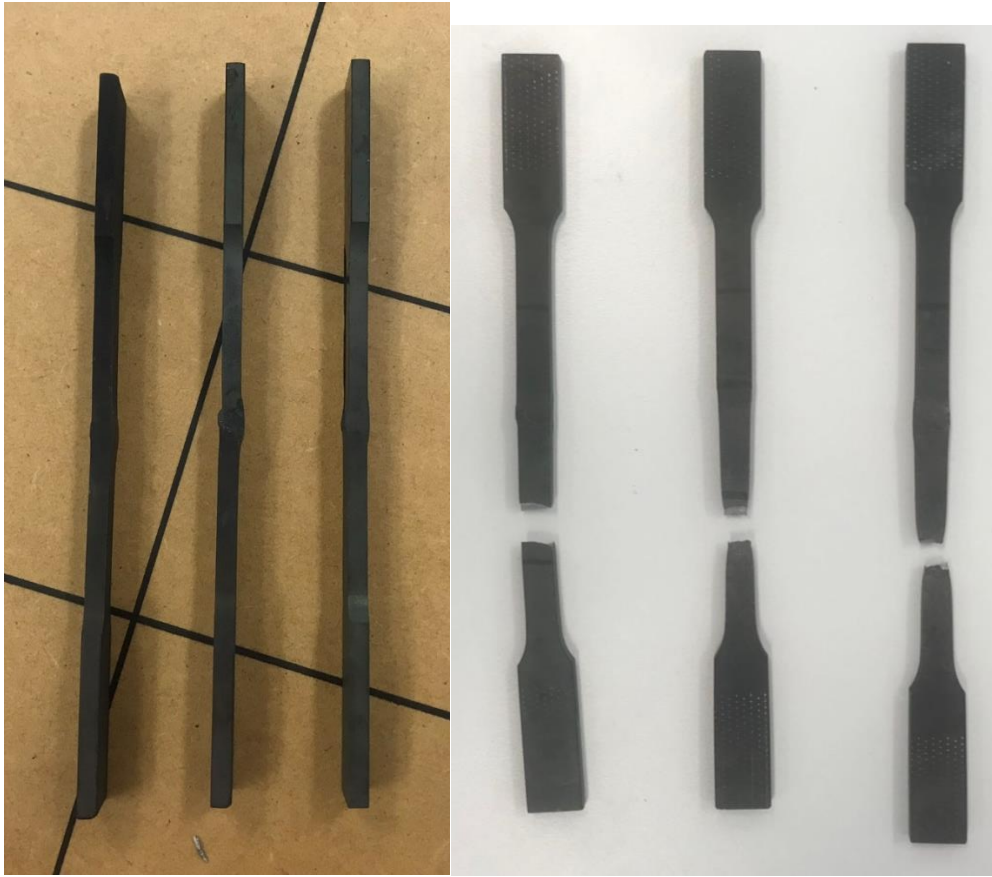


Figure 34 - Air heat treated dogbone samples both before (left) and after (right) fracture.



Figure 35 - PCM heat treated dogbone samples both before (left) and after (right) fracture.

8.3 Vickers Hardness testing

Table 9 – Average hardness of all fractured dissimilar weld samples, without polishing.

Treatment type	Position 1 hardness (HV)	Position 2 hardness (HV)	Position 4 hardness (HV)	Position 6 hardness (HV)	Position 7 hardness (HV)
Pristine	428	314	245	266	461
Argon heated	507	495	336	477	575
Heated in air	424	406	310	253	568
PCM heat treated	140	198	277	148	104

Table 10 – Hardness of dissimilar weld small samples with different treatments after polishing.

Treatment Type	Tests	Position 1 hardness (HV)	Position 2 hardness (HV)	Position 3 hardness (HV)	Position 4 hardness (HV)	Position 5 hardness (HV)	Position 6 hardness (HV)	Position 7 hardness (HV)
Pristine	Test 1	-	-	288	242	225	222	-
	Test 2	-	-	-	-	-	-	-
	Test 3	252	260	233	240	198	191	188
	Test 4	-	-	-	-	-	-	-
	Test 5	-	-	270	240	218	209	-
Argon heated	Test 1	-	-	325	260	226	232	-
	Test 2	-	-	-	-	-	-	-
	Test 3	280	286	292	274	269	203	180
	Test 4	-	-	-	-	-	-	-
	Test 5	-	-	318	280	296	201	-
Heated in air	Test 1	333	277	222	238	237	178	197
	Test 2	289	296	266	252	247	174	181
	Test 3	284	247	262	254	235	183	178
	Test 4	286	261	244	245	238	249	184
	Test 5	370	257	257	256	252	246	183
PCM heat treated	Test 1	-	-	331	218	245	239	-
	Test 2	-	-	-	-	-	-	-
	Test 3	298	295	310	302	291	218	200
	Test 4	-	-	-	-	-	-	-
	Test 5	-	-	330	322	273	220	-

Table 11 - Hardness of similar weld stainless steel 316L small samples with different treatments after polishing.

Treatment Type	Tests	Position 4 hardness (HV)	Position 5 hardness (HV)	Position 6 hardness (HV)	Position 7 hardness (HV)
Pristine	Test 1	198	-	212	-
	Test 3	184	192	199	188
	Test 5	202	-	185	-
Argon heated	Test 1	196	-	217	-
	Test 3	213	204	184	192
	Test 5	215	-	184	-
Heated in air	Test 1	204	217	194	187
	Test 3	189	182	175	168
	Test 5	200	194	181	179

Table 12 – Hardness of small samples air heat treated before polishing.

Sample Type	Tests	Position 1 hardness (HV)	Position 2 hardness (HV)	Position 3 hardness (HV)	Position 4 hardness (HV)	Position 5 hardness (HV)	Position 6 hardness (HV)	Position 7 hardness (HV)
316L - 316L	Test 1	-	-	-	362	260	318	275
	Test 2	-	-	-	307	270	276	258
	Test 3	-	-	-	277	266	272	322
	Ave	-	-	-	315	265	289	285
625 - 625	Test 1	497	314	NA	281	-	-	-
	Test 2	464	472	396	312	-	-	-
	Test 3	410	283	404	408	-	-	-
	Ave	457	356	400	334	-	-	-
316L - 625	Test 1	474	344	NA	341	NA	278	252
	Test 2	519	372	346	NA	244	273	247
	Test 3	464	404	395	340	NA	322	293
	Ave	486	373	371	341	244	291	264

Table 13 – Hardness of small samples air heat treated after polishing.

Sample Type	Tests	Position 1 hardness (HV)	Position 2 hardness (HV)	Position 3 hardness (HV)	Position 4 hardness (HV)	Position 5 hardness (HV)	Position 6 hardness (HV)	Position 7 hardness (HV)
316L -	Test 1	-	-	-	204	217	194	187
316L	Test 2	-	-	-	204	203	195	178
	Test 3	-	-	-	189	182	175	168
	Test 4	-	-	-	179	204	181	174
	Test 5	-	-	-	200	194	177	179
	625 -	Test 1	288	317	314	296	-	-
625	Test 2	300	300	304	294	-	-	-
	Test 3	271	274	279	294	-	-	-
	Test 4	285	283	287	277	-	-	-
	Test 5	298	277	272	279	-	-	-
	316L -	Test 1	333	277	222	238	237	178
625	Test 2	289	296	266	252	247	174	181
	Test 3	284	247	262	254	235	183	178
	Test 4	286	261	244	245	238	249	184
	Test 5	370	257	257	256	252	246	183

Table 14 – Hardness of different polished treated dissimilar weld samples after fracture.

Treatment type	Tests	Position 2 hardness (HV)	Position 4 hardness (HV)	Position 6 hardness (HV)
Pristine	Test 1	283	285	300
	Test 2	274	253	290
	Test 3	253	251	281
	Ave	270	263	290
Argon heated	Test 1	306	310	290
	Test 2	319	314	304
	Test 3	271	259	298
	Ave	299	294	297
Heated in air	Test 1	304	288	281
	Test 2	300	247	347
	Test 3	271	244	528
	Ave	292	260	385

Table 15 – Hardness of different treated dissimilar weld samples after fracture. No polishing process applied.

Treatment type	Tests	Position 1 hardness (HV)	Position 2 hardness (HV)	Position 4 hardness (HV)	Position 6 hardness (HV)	Position 7 hardness (HV)
Pristine	Test 1	407	304	267	279	550
	Test 2	413	393	254	276	437
	Test 3	464	245	214	242	396
	Ave	428	314	245	266	461
Argon heated	Test 1	499	537	476	523	499
	Test 2	488	468	221	514	783
	Test 3	533	480	310	393	442
	Ave	507	495	336	477	575
Heated in air	Test 1	514	376	323	NA	575
	Test 2	376	435	312	261	771
	Test 3	381	408	296	245	357
	Ave	424	406	310	253	568
PCM heat treated	Test 1	125	107	279	154	150
	Test 2	172	92	323	196	85
	Test 3	124	396	228	95	77
	Ave	140	198	277	148	104

Table 16 - Hardness values for different treated stainless steel 316L similar weld fractured samples. No polishing process applied.

Treatment type	Tests	Position 1 hardness (HV)	Position 2 hardness (HV)	Position 4 hardness (HV)	Position 6 hardness (HV)	Position 7 hardness (HV)
Pristine	Test 1	316	311	307	294	395
	Test 2	381	420	379	363	246
	Test 3	354	287	442	314	372
	Ave	350	339	376	324	338
Argon heated	Test 1	335	342	348	337	313
	Test 2	449	494	417	389	303
	Test 3	395	474	418	428	NA
	Ave	393	437	394	385	308
Heated in air	Test 1	328	271	344	310	495
	Test 2	343	354	311	185	372
	Test 3	281	349	282	305	383
	Ave	317	325	312	267	417
PCM heat treated	Test 1	230	NA	196	317	327
	Test 2	265	NA	162	362	117
	Test 3	NA	227	144	231	352
	Ave	248	227	167	303	265

Table 17 - Hardness values for different treated stainless steel 316L similar weld fractured samples. No polishing process applied.

Treatment type	Tests	Position 1 hardness (HV)	Position 2 hardness (HV)	Position 4 hardness (HV)	Position 6 hardness (HV)	Position 7 hardness (HV)
Pristine	Test 1	478	373	592	537	420
	Test 2	439	405	327	557	410
	Test 3	430	535	387	464	442
	Ave	449	438	435	519	424
Argon heated	Test 1	505	422	428	446	523
	Test 2	510	451	499	486	493
	Test 3	530	565	517	480	508
	Ave	515	479	481	471	508
Heated in air	Test 1	432	392	444	488	442
	Test 2	425	446	312	471	448
	Test 3	442	393	354	488	423
	Ave	433	410	370	482	437

Table 18 - Fractured samples hardness values where points get 1 mm closer to weld. Taken from position 2.

Sample	Furthest from weld (HV)	Middle (HV)	Closest to weld (HV)
316L - 625 pristine	304	335	342
316L – 316L Argon	226	277	296
625 – 625 Air	381	360	374

Table 19 - Hardness values of fractured PCM heat treated, similar weld Inconel 625 samples, underneath the broken oxidised surface.

Tests	Position 1 hardness (HV)	Position 2 hardness (HV)	Position 4 hardness (HV)
Test 1	753	647	NA
Test 2	298	605	575
Test 3	647	605	803

Table 20 - Pre fracture PCM hardness values.

Sample Type	Tests	Position 1 hardness (HV)	Position 2 hardness (HV)	Position 3 hardness (HV)	Position 4 hardness (HV)	Position 5 hardness (HV)	Position 6 hardness (HV)	Position 7 hardness (HV)
316L -	Test 1	-	-	-	228	158	133	105
316L	Test 2	-	-	-	262	131	148	308
	Test 3	-	-	-	173	207	308	141
	Ave	-	-	-	221	165	196	185
316L - 625	Test 1	138	124	214	125	244	209	226
	Test 2	230	146	394	157	344	198	141
	Test 3	300	174	139	338	59	144	108
	Ave	223	148	249	207	216	183	158

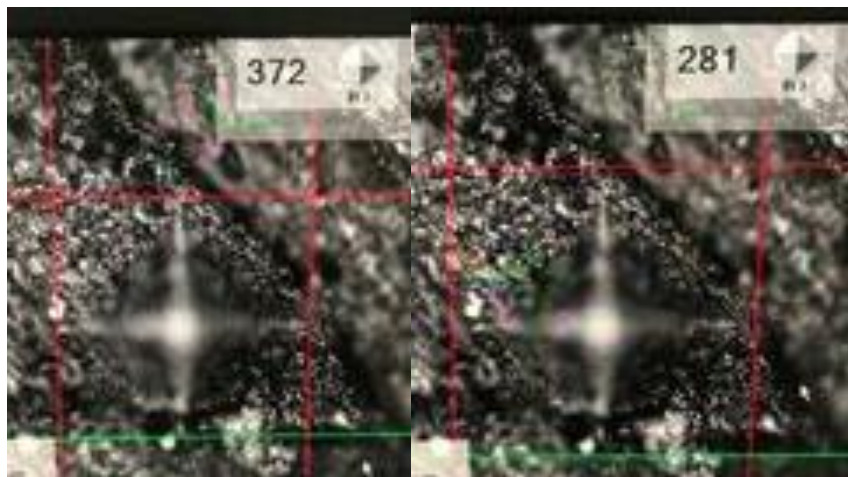


Figure 36 - Example of size differences from the same point due to unpolished surface.



Figure 37 - Example of distortion on unpolished samples.



Figure 38 - Example of slipping in multiple situations, Polished samples (left) PCM heat treated samples (centre) Unpolished samples (right).

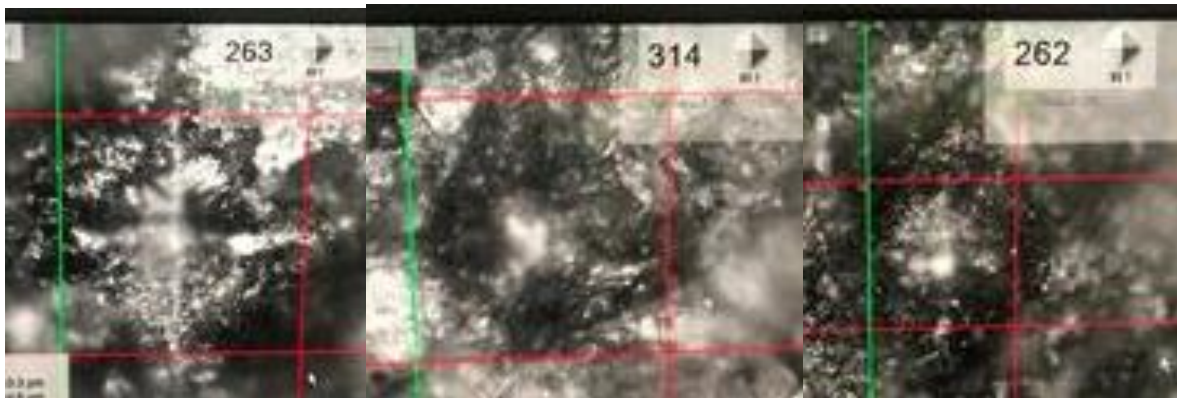


Figure 39 - Images of hardness points from the broken oxidised Inconel strip. 3 separate tested positions.

8.4 Optical microscopy

Table 21 – Topography of pristine dissimilar weld fractured sample, when unpolished.

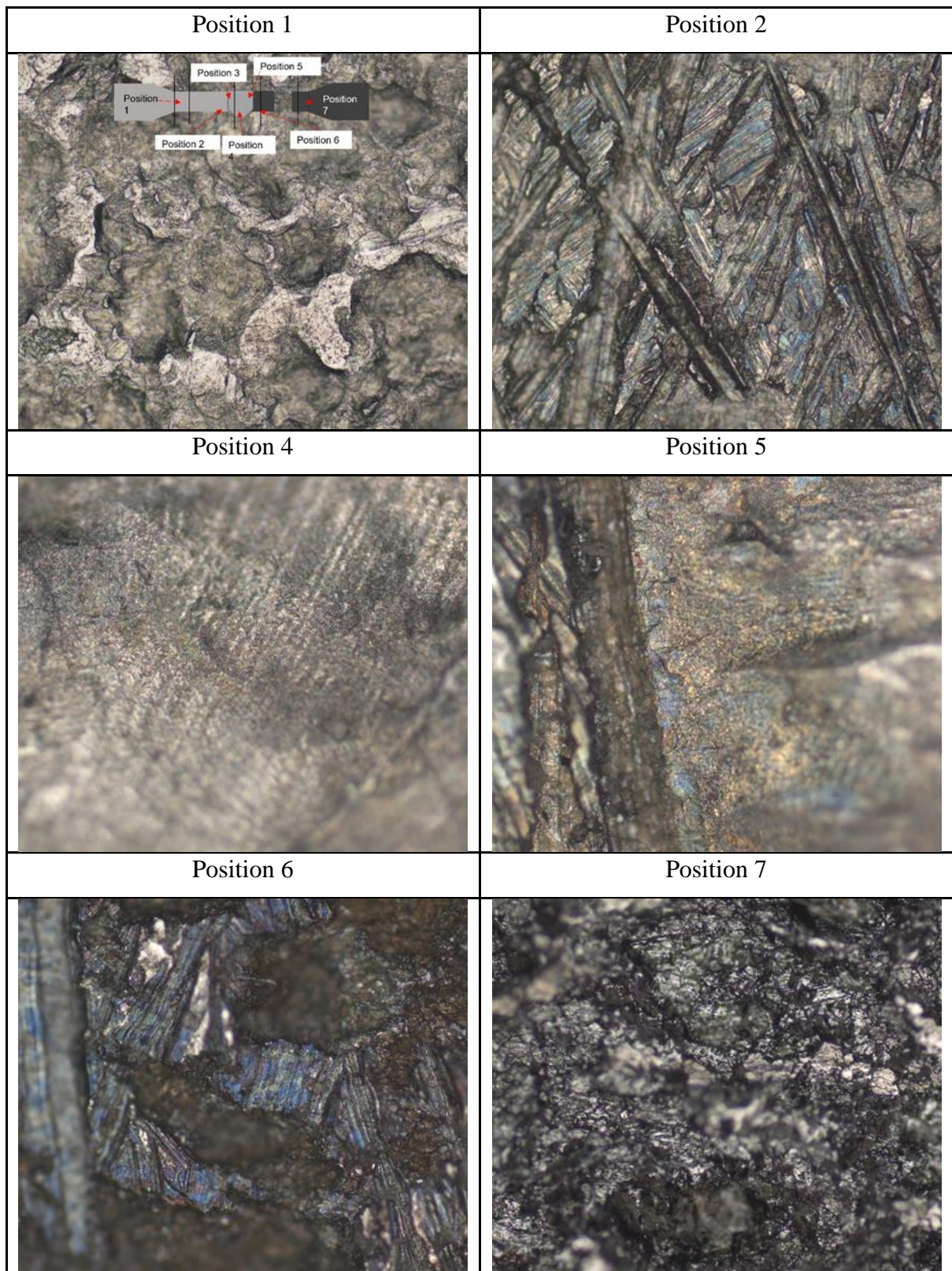


Table 22 – Topography of PCM heat treated dissimilar weld fractured sample, when unpolished.

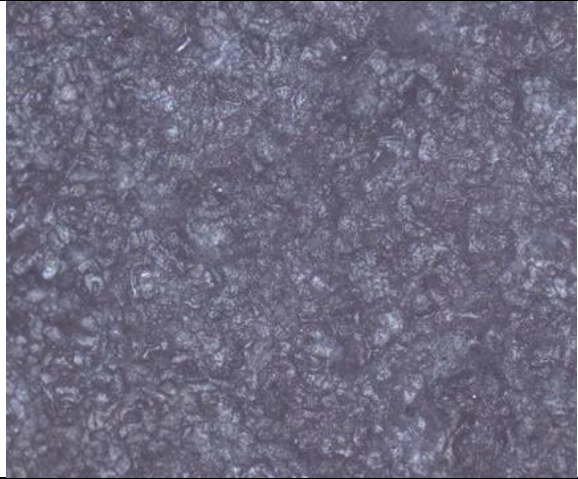
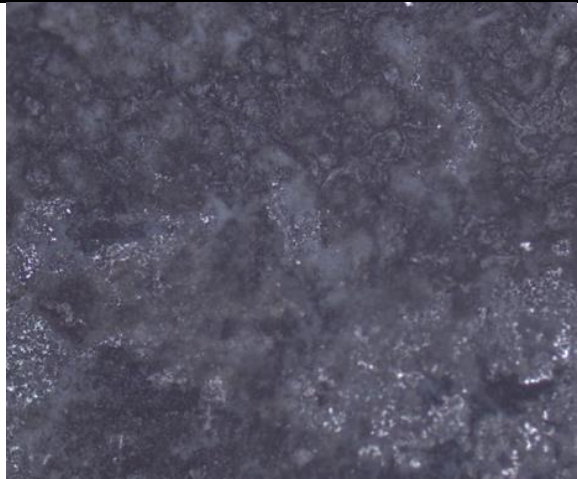
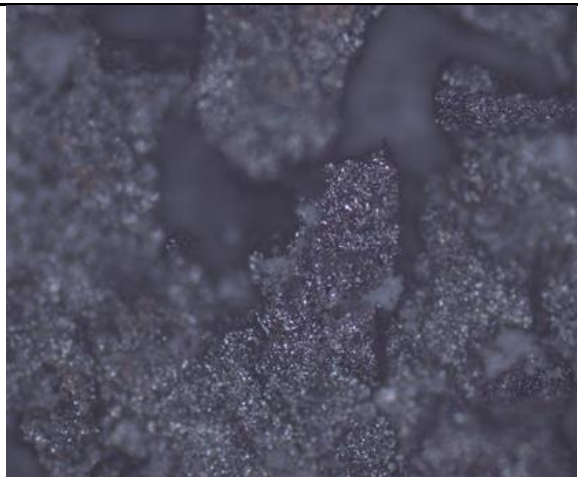
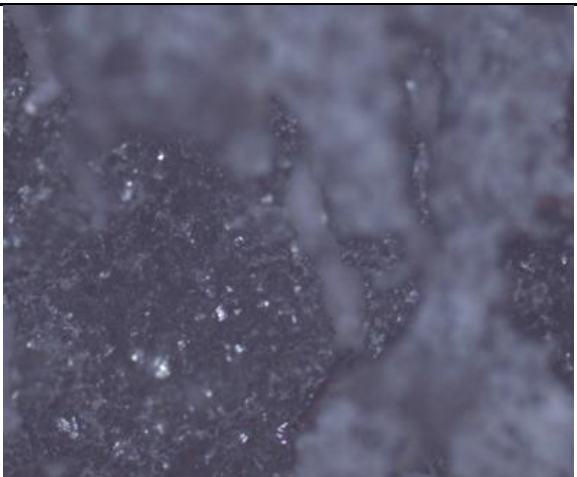
Position 1	Position 2
	
Position 4	Position 5
	NA
Position 6	Position 7
	

Table 23 - Differences in welds of dissimilar weld samples after different treatments of unpolished samples before and after fracture.

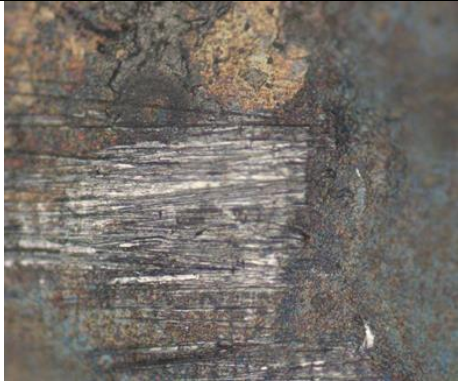
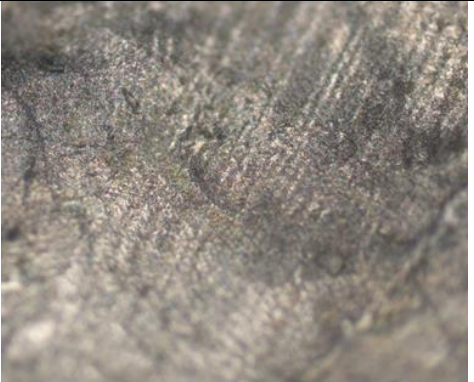
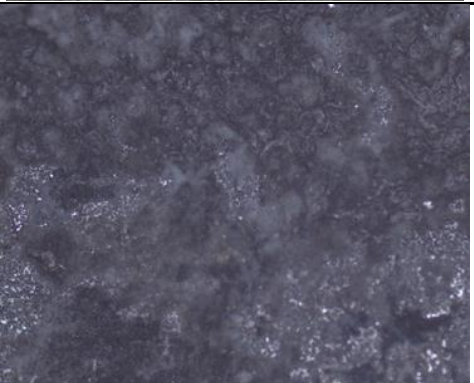
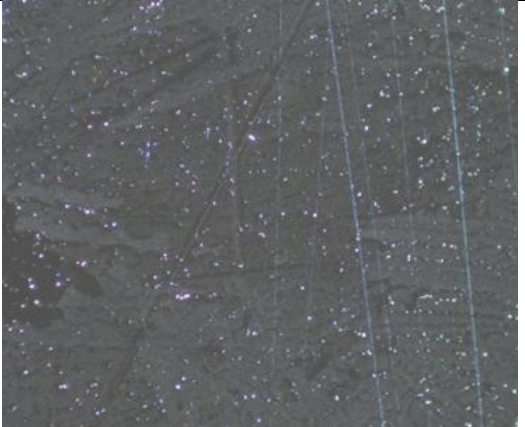
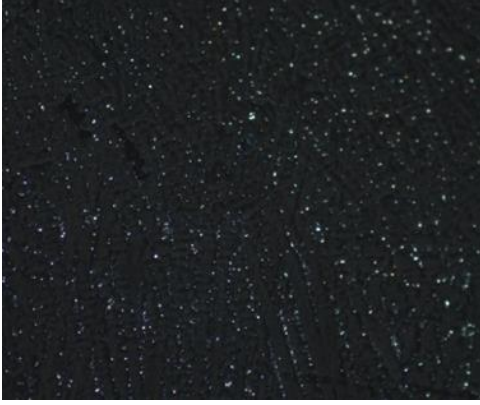
Treatment	Before fracture	After fracture fractured
Pristine		
Argon	NA	
Air		
PCM		

Table 24 - Differences in welds of dissimilar samples after different treatments of polished samples before and after fracture.

Treatment	Before fracture	After fracture
Pristine	NA	
Argon	NA	
Air		

8.5 SEM and EDX

Table 25 - SEM images of polished air heat treated cross section, dissimilar weld samples after fracture.

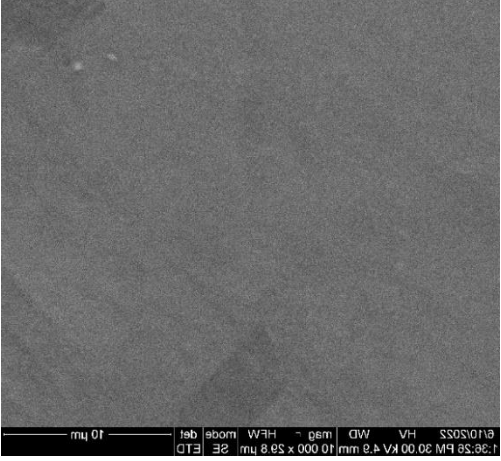
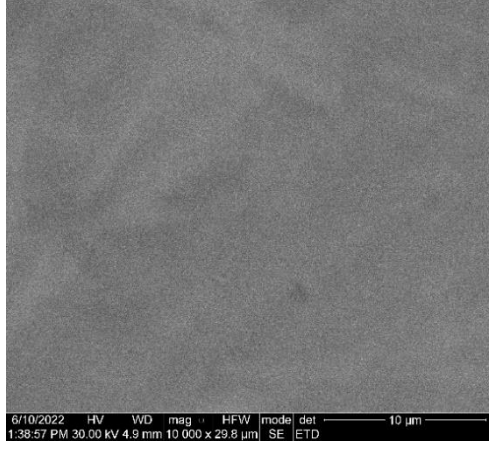
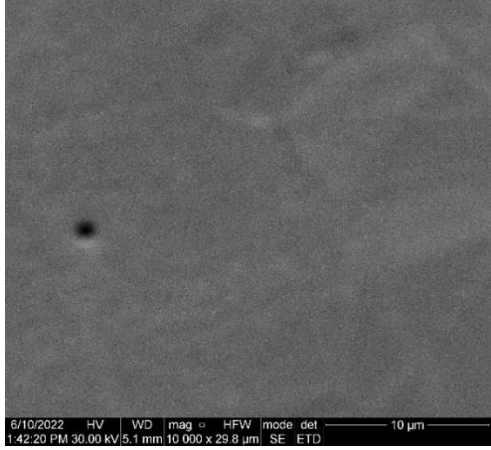
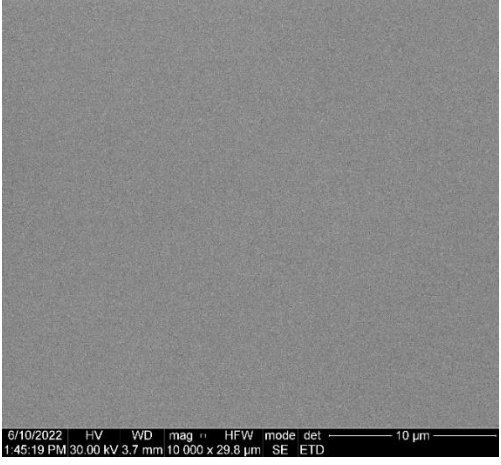
Position 1	Position 2
	
Position 4	Position 6
	
Position 7	
	

Table 26 - Images of unpolished air heat treated dissimilar weld small samples, at different positions.

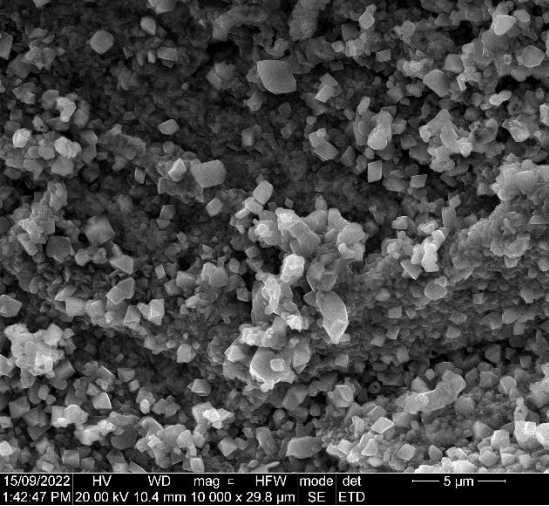
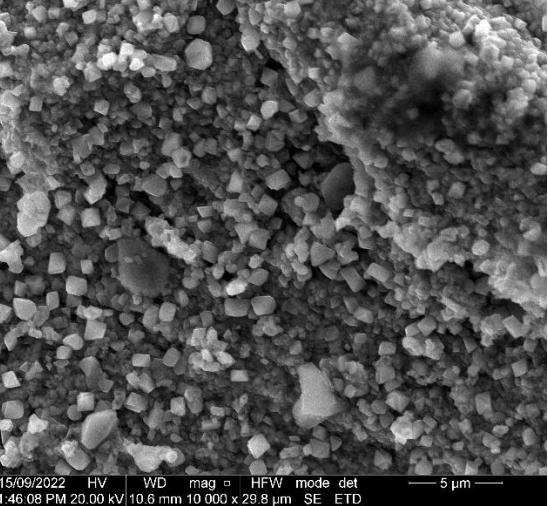
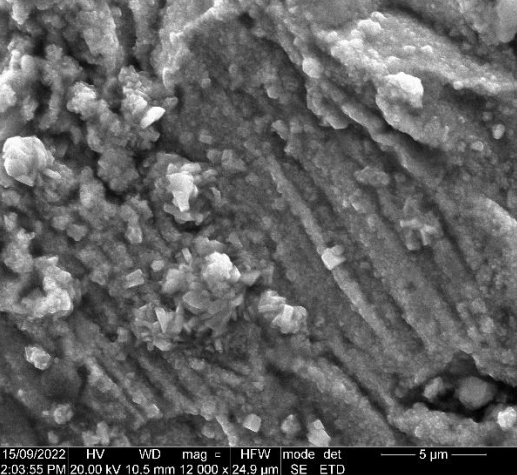
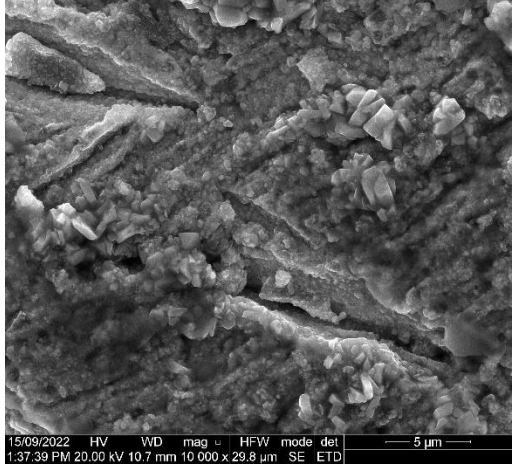
Position 1	Position 2
	
Position 4	Position 6
	
Position 7	
	

Table 27 - Images of unpolished stainless steel 316L similar weld air heat treated small samples, at different positions.

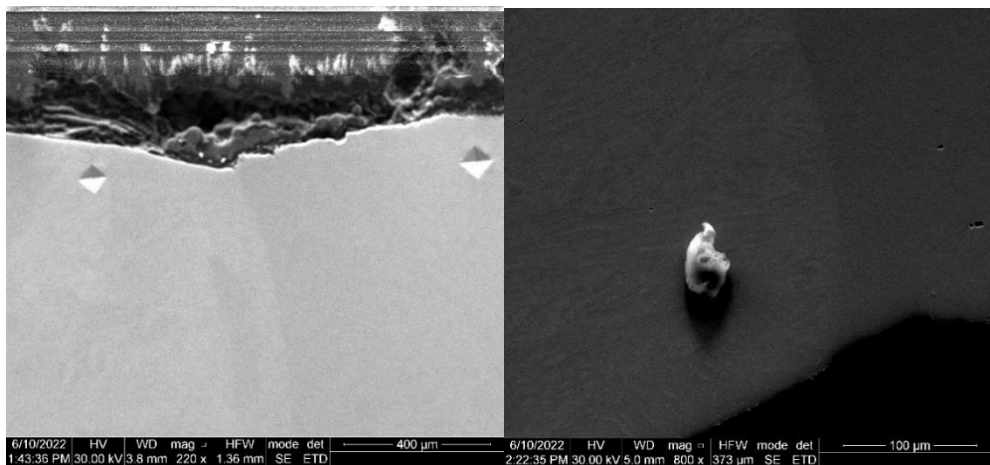
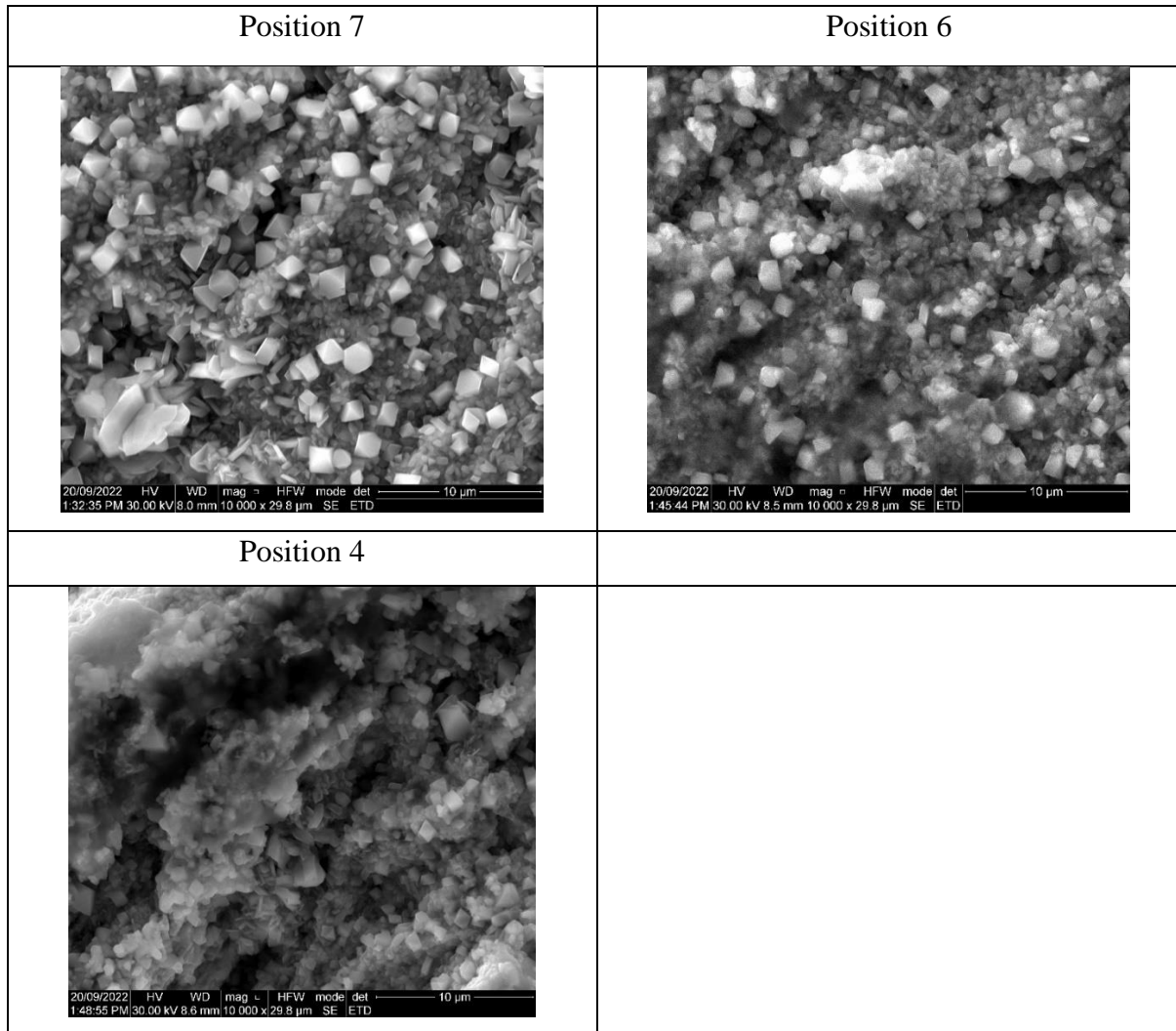


Figure 40 - SEM images small cross section air heat treated samples after fracture located at the weld lines. Butt of weld perspective (left) and long weld perspective (right).

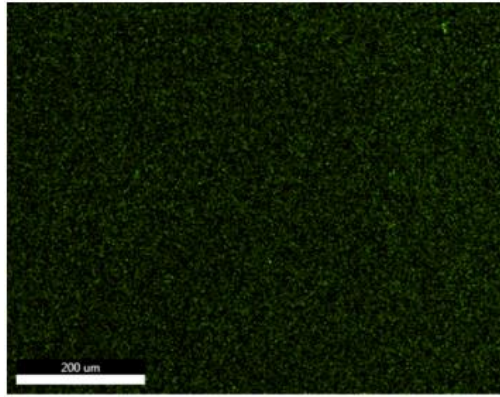


Figure 41 - EDX image of oxygen content below weld line. Air heat treated cross section of small samples.

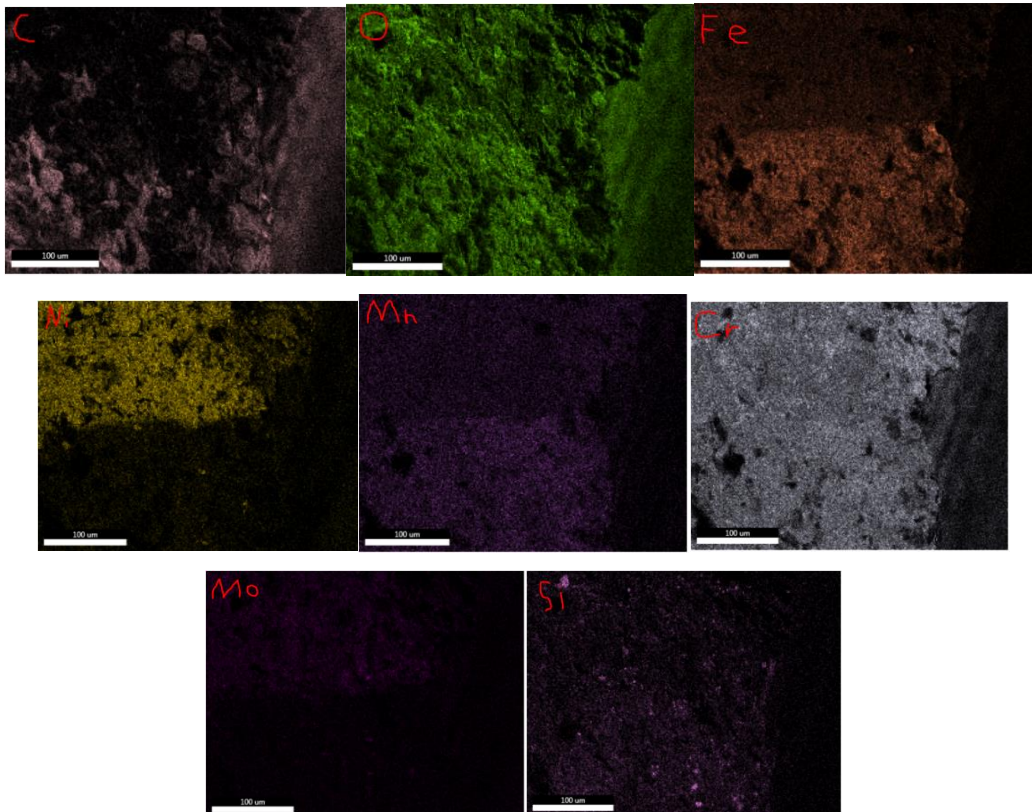
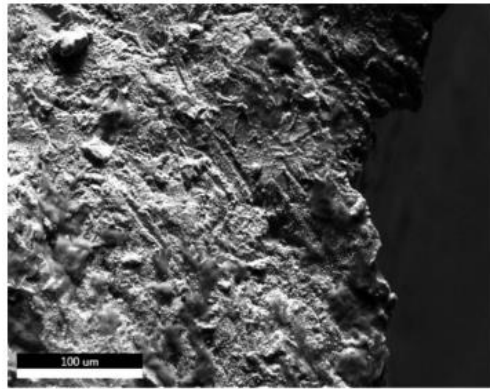


Figure 42 - EDX of dissimilar weld small sample, after air heat treatment with no polishing.

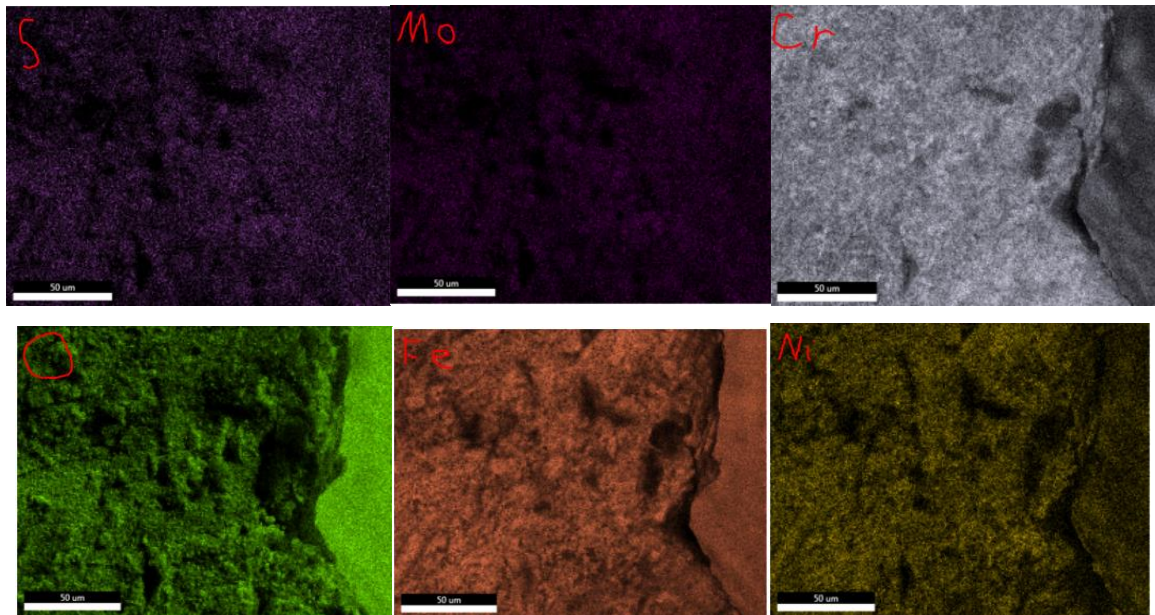
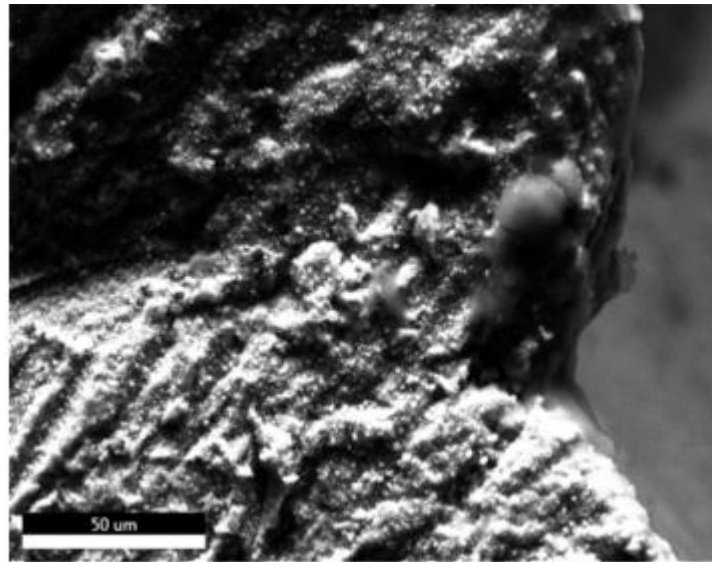


Figure 43 - EDX of stainless steel 316L similar weld small sample, after air heat treatment with no polishing.

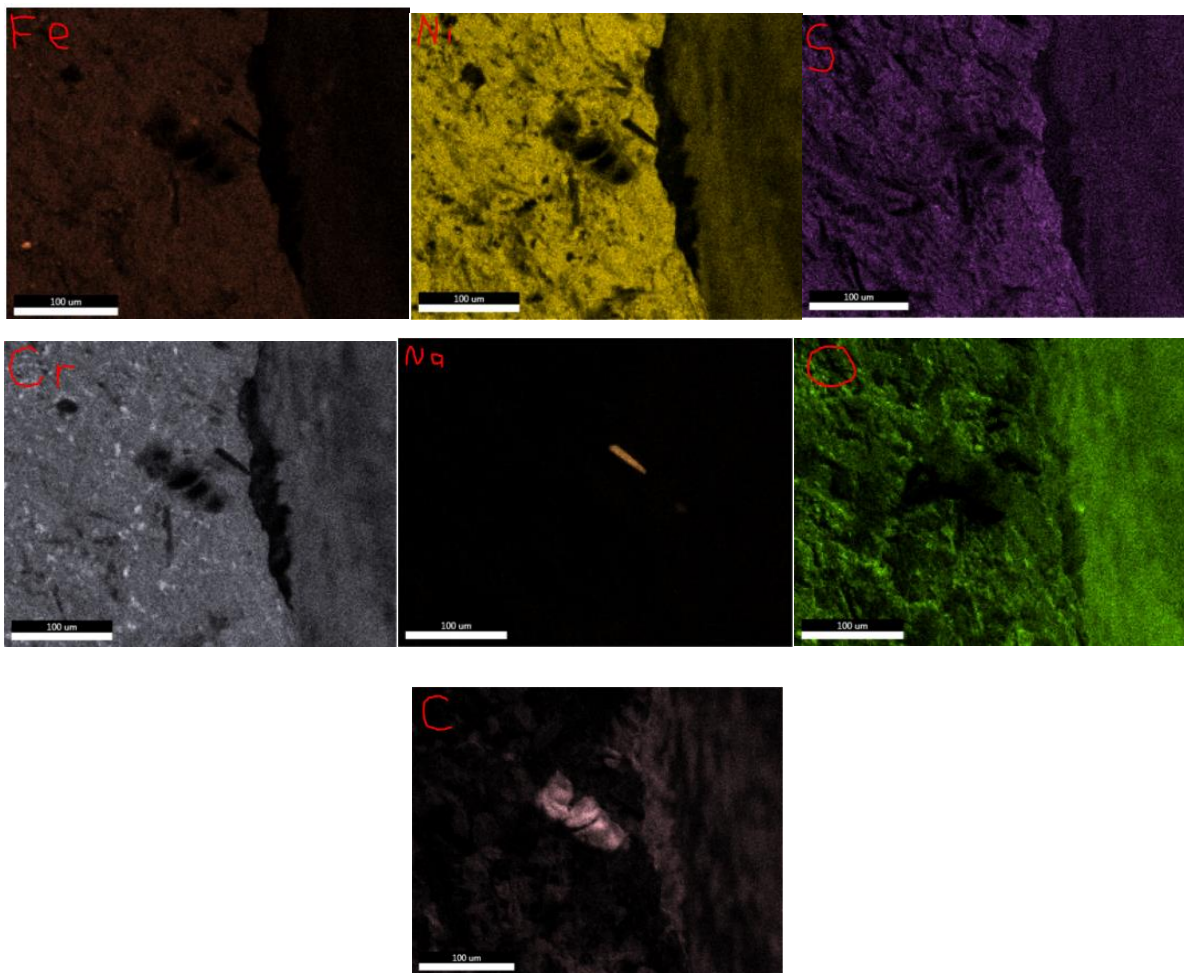
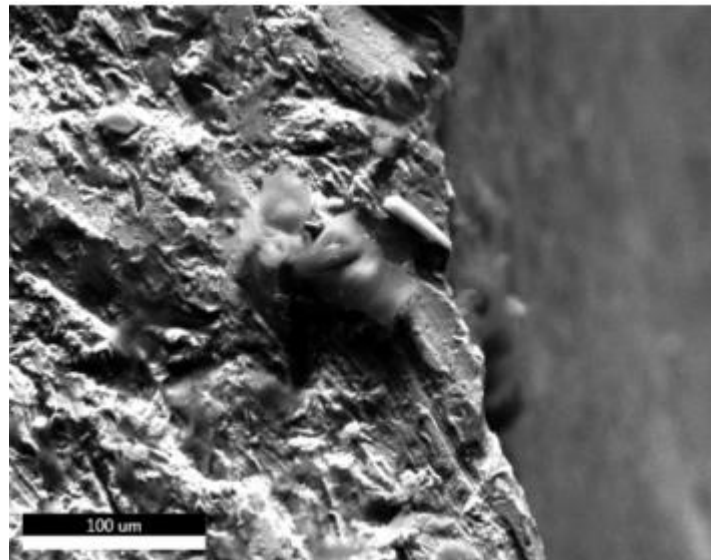


Figure 44 - EDX of Inconel 625 similar weld small sample, after air heat treatment with no polishing.

Table 28 - Material loss estimation on unpolished air heat treated small samples.

Position 1	Position 2
Position 4	Position 6
Position 7	

Table 29 – Material loss average values.

Sample	Sample position	Average layer thickness (um)
Argon HT	Position 1	2
	Position 2	2.3
	Position 4	2.3
	Position 6	2.7
	Position 7	2
Air HT	Position 1	170.5
	Position 2	119.6
	Position 4	109.6
	Position 6	52.6
	Position 7	59.9
PCM HT	Position 1	530
	Position 2	500
	Position 4	590
	Position 6	100
	Position 7	110

Table 30 – Material gain of dissimilar weld samples after each treatment, determined through EDX oxygen levels and visible differences, at the 5 main locations.

Sample	Sample area	Average layer thickness (um)
Argon HT	Position 1	16
	Position 2	22
	Position 4	22
	Position 6	25
	Position 7	16
Air HT	Position 1	500
	Position 2	741
	Position 4	400
	Position 6	200
	Position 7	300
PCM HT	Position 1	4550
	Position 2	4300
	Position 4	4900
	Position 6	900
	Position 7	1050